# Remote Sensing Reflectance and Inherent Optical Properties in the mid-mesohaline Chesapeake Bay

Maria Tzortziou [a *]
Ajit Subramaniam [b]
Jay R. Herman [c]
Charles L. Gallegos [d]
Patrick J. Neale [d]
Lawrence W. Harding Jr, [e]

[a] University of Maryland, Earth System Science Interdisciplinary Center
College Park, MD, 20742, USA

[b] Lamont Doherty Earth Observatory, Columbia University
Palisades, NY, 10964, USA

[c] NASA/Goddard Space Flight Center
Greenbelt, MD, 20771, USA

[d] Smithsonian Environmental Research Center
Edgewater, MD, 21037, USA

[e] University of Maryland, Horn Point Laboratory
Cambridge, MD 21613, USA

[*] Corresponding Author:

e-mail address: martz@carioca.gsfc.nasa.gov (M. Tzortziou)
telephone number: 301 614 6048
fax number: 301 614 5903

Running header: Remote Sensing Reflectance and Inherent Optical Properties in the Chesapeake Bay

Submitted to: Estuarine, Coastal and Shelf Science

**Abstract:**

We used an extensive set of bio-optical data and radiative transfer (RT) model simulations of radiation fields to investigate relationships between inherent optical properties and remotely sensed quantities in the optically complex, mid-mesohaline Chesapeake Bay waters. Field observations showed that the chlorophyll algorithms used by the MODIS (MODerate resolution Imaging Spectroradiometer) ocean color sensor (i.e. Chlor_a, chlor_MODIS, chlor_a_3 products) do not perform accurately in these Case 2 waters. This is because, when applied to waters with high concentrations of chlorophyll, all MODIS algorithms are based on empirical relationships between chlorophyll concentration and blue-green wavelength remote sensing reflectance ($R$rs) ratios that do not account for the typically strong blue-wavelength absorption by non-covarying, dissolved and non-algal particulate components. Stronger correlation was observed between chlorophyll concentration and $R$rs ratios in the red (i.e. $R$rs(677)/$R$rs(554)) where dissolved and non-algal particulate absorption become exponentially smaller. Regionally-specific algorithms that are based on the phytoplankton optical properties in the red wavelength region provide a better basis for satellite monitoring of phytoplankton blooms in these Case 2 waters. Good optical closure was obtained between independently measured $R$rs spectra and the optical properties of backscattering, $b_b$, and absorption, $a$, over the wide range of in-water conditions observed in the Chesapeake Bay. Observed variability in the quantity $f/Q$ (proportionality factor in the relationship between $R$rs and the water inherent optical properties ratio $b_b/(a+b_b)$) was consistent with RT model calculations for the specific measurement geometry and water bio-optical characteristics. Data and model results showed that $f/Q$ values in these Case 2 coastal waters are not considerably different from those estimated in previous studies for Case 1waters. Variation in surface backscattering significantly affected $R$rs magnitude

across the visible spectrum and was most strongly correlated ($R^2$=0.88) with observed variability in *R*rs at 670 nm. Surface values of particulate backscattering were strongly correlated with non-algal particulate absorption, $a_{nap}$, in the blue wavelengths ($R^2$=0.83). These results, along with the measured values of backscattering fraction magnitude and non-algal particulate absorption spectral slope, suggest that suspended non-algal particles with high inorganic content are the major water constituents regulating $b_b$ variability in the mid-mesohaline Chesapeake Bay. Remote retrieval of surface $b_b$ and $a_{nap}$ from *R*rs(670) can be used in regionally-specific satellite algorithms to separate contribution by non-algal particles and dissolved organic matter to total light absorption in the blue, and monitor non-algal suspended particle concentration and distribution in these Case 2 waters.

Keywords: bio-optics; satellite retrievals; radiative transfer; Case 2; estuaries; coastal waters

## 1. Introduction

Changes in the concentrations and distribution of organic and inorganic, particulate and dissolved substances are of major water quality and ecologic concern in the Chesapeake Bay estuary. Increased nutrient loadings in recent years, driven mainly by human population growth and changes in land use, have increased phytoplankton concentrations above historical levels (Harding and Perry, 1997). Changes in particulate and dissolved substances are linked to important processes in the estuary, such as freshwater river discharges, nutrient and light availability in the water column, tidal mixing, bottom resuspension, and microbial activity (e.g. Kemp and Boynton, 1992; Malone, 1992). Because composition and concentrations of seawater constituents influence water optical characteristics, in-situ measurements of optical properties have been made by several ship-based monitoring programs during the last decades to examine water quality and assess progress in reversing eutrophication in the Bay (e.g. Glibert et al., 1995; Johnson et al., 2001). By using appropriate bio-optical algorithms, remote sensing of "ocean color" offers the capability of extending field observations beyond the restricted in-situ sampling domain. Several aircraft ocean-color instruments (using both "passive" and "active" systems) have been used to remotely measure surface chlorophyll-a concentrations [chl-a] and determine changes in phytoplankton biomass in the Chesapeake Bay (e.g. Hoge and Swift, 1981; Harding et al., 1992; Lobitz et al., 1998). However, only a limited number of studies has been published on the interpretation of satellite ocean color imagery and the applicability of currently used satellite algorithms for these optically complex estuarine waters (e.g. Harding et al., 2005).

In order to use satellite ocean color to extract information on water composition it is necessary to develop effective bio-optical algorithms relating the remotely sensed water reflectance either directly to surface concentrations of optically active water constituents

(empirical algorithms; e.g. Clark, 1997; O'Reilly et al., 2000), or to their optical properties based on principles derived from radiative transfer theory (semi-analytical inversion models; e.g. Garver and Siegel, 1997; Maritorena et al., 2002). Since the launch of the Coastal Zone Color Scanner (CZCS) in October 1978, satellite ocean color has contributed significantly to gaining a better understanding of biological activity in open-ocean "Case 1" waters where phytoplankton and co-varying material are the major optical components (e.g. Yentsch, 1993; Longhurst et al., 1995; Gregg and Conkright, 2001). With more channels in the visible part of the spectrum, CZCS's follow-on sensor SeaWiFS (Sea-viewing Wide Field of view Sensor; launched in 1997) and the newer instrument MODIS (MODerate resolution Imaging Spectroradiometer, launched in 1999) allowed for further improvements in satellite retrievals of biogeochemical variables in Case 1 waters (e.g. Yoder and Kennelly, 2003; Carder et al., 2004; McClain et al., 2004). A more difficult challenge, however, has been developing bio-optical algorithms suitable for use in optically complex "Case 2" waters, like the Chesapeake Bay, where multiple, co-existing but not necessarily co-varying, dissolved and particulate, marine and terrigenous substances affect ocean color (e.g. Morel and Prieur, 1977; Carder et al., 1991; Darecki and Stramski, 2004).

Harding et al. (2005) used SeaWiFS [chl-a] data and in-situ measurements of water reflectance and [chl-a] to examine the accuracy of satellite observations and the applicability of the SeaWiFS empirical chlorophyll algorithm OC4v4 (O'Reilly et al., 2000) for the Chesapeake Bay and Middle Atlantic Bight. They found that SeaWiFS reliably captured seasonal and inter-annual variability of phytoplankton biomass in the lower Bay. However, the OC4v4 algorithm significantly overestimated chlorophyll in the mid-mesohaline and upper Chesapeake Bay, due to strong absorption by dissolved organic matter and non-algal particles that are not sufficiently accounted for in this empirical chlorophyll algorithm (Harding et al., 2005).

These studies underscore the need to develop more accurate Case 2 algorithms based on detailed in-situ bio-optical characteristics. However, certain optical properties of the Chesapeake Bay remain poorly characterized. Magnuson et al. (2004) used an extensive set of bio-optical data to examine the parameterization and validation of the semi-analytical Garver-Siegel-Maritorena (GSM01) model (Maritorena et al., 2002) for application in the Chesapeake Bay and the Mid-Atlantic Bight. A major limitation in their efforts was that information on the backscattering ($b_b$) characteristics of Chesapeake Bay is extremely scarce. Due to the lack of in-situ data, modeling of $b_b$ is often based on assumptions regarding scattering angular shape, backscattering magnitude and spectral dependence. According to Magnuson et al. (2004) the lack of $b_b$ measurements in the Bay affected backscattering parameterizations in their study and posed a significant limitation on the evaluation of the GSM01 model's backscattering product. Tzortziou et al. (submitted) recently applied detailed in-situ data and radiative transfer simulations to examine $b_b$ variability and modeling of backscattering processes for the mid-mesohaline Chesapeake Bay. Information is scarce on the contribution of various water constituents to the backscattering characteristics of Chesapeake Bay, and the application of remotely sensed ocean color data to the remote retrieval of particulate backscattering variability in these Case 2 waters.

Previous studies have shown that the remote sensing reflectance $R$rs, defined as the upwelling radiance emerging from the ocean divided by the downwelling irradiance reaching the water surface, is, to a first approximation, proportional to the ratio of water backscattering, $b_b$, and absorption, $a$, coefficients, $b_b/(a+b_b)$ (e.g. Morel and Prieur, 1977). However, the magnitude and geometrical structure (or shape) of the upwelling radiance field within the ocean depend on both the water inherent optical properties (IOPs; e.g. volume scattering function (VSF), $b_b$, $a$), as

well as on the processes and environmental variables (e.g. solar zenith angle, aerosol load, surface waves) that affect illumination conditions (Austin, 1974; Morel and Gentili, 1991; 1993). Measurements, theoretical studies, and radiative transfer computations of the effects of these parameters on the relationship between $R$rs and the IOPs ratio $b_b/(a+b_b)$ have been performed for Case 1 waters (e.g. Voss, 1989; Morel and Mueller, 2002; Voss and Morel, 2005). Further studies are needed for Case 2 waters, like the Chesapeake Bay, that are characterized by high bio-optical complexity.

In this paper, we use radiative transfer (RT) modeling and detailed in-situ bio-optical measurements, including new data on particulate backscattering, to examine relationships between remotely sensed $R$rs spectra and IOPs for improved remote retrievals of biogeochemical variables in the mid-mesohaline Chesapeake Bay. Our main objectives were to: (i) assess the applicability of the chlorophyll algorithms currently used by SeaWiFS' successor MODIS, and examine alternative chlorophyll algorithms based on the red wavelengths where absorption by non-algal particles and dissolved matter are minimal; (ii) evaluate variability in the relationship between $R$rs and $b_b/(a+b_b)$ for our measurement geometry, and compare our observations with RT calculations for Case 2 waters and previous studies for Case 1 waters; (iii) determine the relative roles of different particulate substances in light backscattering in the mid-mesohaline Chesapeake Bay, and examine methods for remote retrieval of surface $b_b$ and suspended particles in these waters.

## 2. Theoretical background

Remote sensing of ocean color relies on detecting the light signal that leaves the water surface and reaches a sensor onboard a satellite, carrying with it information on water IOPs. The magnitude of the ocean remote sensing reflectance $R$rs is related to the processes of

backscattering, which redirects downwelling photons to travel upward and eventually leave the water surface, and absorption, which converts photons energy to other forms of energy such as heat or chemical energy. As upward traveling photons exit the water they interact with the air-water interface by refraction and internal reflection. *R*rs can, therefore, be related to backscattering and absorption according to (e.g. Austin, 1974; Preisendorfer, 1976; Gordon et al., 1975; 1988; Lee et al., 1994):

$$Rrs(\lambda) = \frac{f}{Q} \cdot \frac{t_{(w,a)} t_{(a,w)}}{n_w^{\,2}} \cdot \frac{b_b(\lambda)}{\alpha(\lambda) + b_b(\lambda)} \qquad (1)$$

where, $b_b(\lambda)$ is the total backscattering coefficient at wavelength $\lambda$, $a(\lambda)$ is the total absorption coefficient, $t_{(w,a)}$ is the water-air transmittance, $t_{(a,w)}$ is the transmittance from air to water, and $n_w$ is the real part of the water refractive index. The quantity $f$ is a complex function of wavelength, water IOPs (single scattering albedo and volume scattering function), solar zenith angle ($\theta_o$), aerosol optical thickness, and wind speed (Gordon et al., 1975; Kirk, 1984; Morel and Mueller, 2002). The quantity $Q$ is defined as the ratio of upwelling irradiance to upwelling radiance, $Q = Eu(\lambda)/Lu(\lambda)$ (Austin, 1974). Therefore, $Q$ is influenced by the processes and environmental variables that affect the geometrical structure of the anisotropic upward radiance field (i.e. IOPs and environmental variables mentioned above, direction of upward traveling photons, and azimuth angle) (Morel and Mueller, 2002).

Variability in the ratio $f/Q$ and its implications in ocean color remote sensing have been the focus of several theoretical and RT computational studies. Early studies showed that the quantity $f$ has an average value of about 0.32–0.33 (Gordon et al., 1975; Morel and Prieur, 1977) when the sun is near zenith. However, according to Morel and Mueller (2002) the global range of variation in $f$ is from about 0.3 to 0.6. Morel and Gentili (1993) found that $Q$ values generally

range from 3 to 6. According to their study, both the $f$ and $Q$ functions experience concomitant increases when the sun zenith angle increases. Therefore, the $f/Q$ ratio would be expected to be less dependent on solar zenith angle than either $f$ or $Q$ alone. Studies by Morel and Gentili (1993) and Gordon et al., (1988) have shown that the ratio $f/Q$ is relatively independent of solar zenith angle for sun and viewing angles expected for the MODIS orbit, with average $f/Q$ = 0.0936, 0.0944, 0.0929, and 0.0881, (SD = 0.005), for $\lambda$= 440, 500, 565, and 665 nm, respectively according to Morel and Gentili (1993), and $f/Q$ = 0.0949, for $\theta_o < 20^o$ according to Gordon et al. (1988). Thus, in various bio-optical algorithms that relate $R$rs to IOPs, $f/Q$ is assumed to be independent of wavelength and solar zenith angle (e.g. the MODIS semi-analytical chlorophyll algorithm; Carder et al., 2002).

Using detailed RT computations Morel and Mueller (2002) showed that $f/Q$ varies within the range 0.08 - 0.15. For simplicity, Morel and Mueller performed their RT calculations for homogeneous Case 1 waters, which allowed them to model all water IOPs ($a$, $b_b$, and VSF) as a function of the chlorophyll-a concentration (Morel et al., 2002). Their theoretical computations of $Q$ showed very good agreement with measurements of radiance distribution performed by Voss and Morel (2005) over a large range of chlorophyll concentrations in the Case 1 waters of Baja California. The degree of agreement between theoretical computations and measurements of $f/Q$ variability in Case 2 waters, however, remains unknown. One of the main objectives in this paper is to examine variability in the quantity $f/Q$ and, as a result, in the relationship of $R$rs : $b_b/(a+b_b)$, for the geometry of our measurements, and over a wide range of bio-optical and environmental conditions for the Case 2 Chesapeake Bay waters.

## 3. Methods

### *3.1. Location and duration of measurements*

Measurements of water inherent optical properties and radiation fields were performed at four stations designated: Poplar Island (PI), Herring Bay (HB), Tilghman Island (TI), and Jetta (JT), in the mid-mesohaline Chesapeake Bay estuary, on the eastern coast of the US (38.71° - 38.89° N latitude, 76.34° - 76.54° W longitude) (Figure 1). Measurements were made during 17 cruises performed in the spring, summer, and fall months between June 2001 and November 2002 (Table 1).

### *3.2. In-situ and laboratory measurements of water optical characteristics*

In-situ vertical profiles of total (minus pure water) attenuation, $c_{t\text{-}w}(\lambda, z)$, and absorption, $a_{t\text{-}w}(\lambda, z)$, were measured at nine visible wavelengths using a WETLabs Spectral AC-9 (Table 2). Temperature and salinity were measured with Hydrolab Datasonde 4a, and these data were used to correct AC9 measurements for the temperature and salinity dependence of absorption by pure water (Pegau et al., 1997). Total particulate scattering, $b_p(\lambda, z)$, was estimated as the difference between $c_{t\text{-}w}(\lambda, z)$ and $a_{t\text{-}w}(\lambda, z)$, after applying additional corrections to account for scattering losses manifested as overestimates of measured absorption (Kirk, 1992; Tzortziou et al., 2004). An ECOVSF3 instrument (WetLabs Inc; Moore et al., 2000) was used to measure backscattering at three angles (100°, 125°, 150°) and three visible wavelengths (450, 530, 650 nm). Measurements were corrected for attenuation and were integrated (90-180°) to obtain the total backscattering coefficient according to manufacturer's instructions. Measurements by Boss et al. (2004) in the Case 2 waters off the coast of New Jersey showed that estimates of $b_b$ using an ECOVSF3 instrument were in very good agreement ($R^2$=0.99) with $b_b$ measurements using a

HOBILabs Hydroscat-6 (Maffione and Dana, 1997). These results increase confidence on the accuracy of the backscattering measurements technique, especially since the instruments have large differences in design and calibration (Boss et al. 2004).

Water samples collected from discrete depths were filtered using 0.22 μm pore-diameter polycarbonate membrane filters (Poretics) to separate the dissolved material. Suspended particulate matter was collected on 25 mm glass fiber filters (Whatman GF/F). Absorbance spectra of chromophoric dissolved organic matter (CDOM), phytoplankton, and non-algal particulate matter were measured using a Cary-IV dual-beam spectrophotometer using the approach of Gallegos and Neale (2002). Particulate absorbance spectra were corrected for scattering errors using a pathlength amplification factor estimated empirically by comparing particulate optical density measured on filters and in particle suspension (Mitchell et al., 2000; Tzortziou, 2004). Absorption spectral slope coefficients, describing the exponential decline of absorption with increasing wavelength for CDOM, $S_{CDOM}$, and non-algal particulate matter, $S_{nap}$, were determined by applying non-linear least-squares regression to the absorption coefficients versus wavelength (290-750 nm) (Blough and Del Vecchio, 2002). Chlorophyll-a concentrations were measured spectrophotometrically in 90% acetone extracts of seston collected on 47 mm GF/F glass fiber filters (Jeffrey and Humphrey, 1975).

### *3.3. In-situ data and theoretical estimations of radiation fields*

Two sensor arrays were used to measure underwater radiation fields in this work, depending on instrument availability. On eight cruises (Table 1) underwater upwelling, $E_u(z)$, and downwelling, $E_d(z)$, spectral irradiance profiles, and above-water surface downwelling irradiance, $E_s$, were measured using Satlantic OCI-200 seven-channel irradiance sensors (Table 2). The irradiance sensors were mounted on a custom frame so that up- and down-welling

sensors were almost coplanar. On the rest of our cruises we used a Satlantic MicroPro free-falling radiometer (Table 1) to measure water column profiles of upwelling radiance, $Lu(z)$, and $Ed(z)$ in the water column, and Satlantic OCR-507 Surface Reference Irradiance sensors for measurements of $Es$, at 14 wavebands (Table 2) . The optical heads of MicroPro have relatively small diameters (6.4 cm) compared to other radiometric instruments and are less subject to instrument self-shading (Harding and Magnuson, 2002). The instrument contains a pressure sensor that gives depth, and a miniature biaxial clinometer for tilt measurements (accuracy of $0.2^{o}$) (Satlantic MicroPro operation manual, 2002).

When using the Micropro, three casts were made at each station, and all casts were completed within 5-8 minutes. Measurements that did not meet quality control (e.g. casts characterized by large tilt-angles or changing cloudiness conditions) were omitted from analysis. In cases when more than one cast were of good quality $Lu$ was estimated as the average of all casts. Measurements of $Lu(z)$ were corrected for instrument self-shading errors (Gordon and Ding, 1992; Zibordi and Ferrari, 1995) and for the depth offset between the $Ed$ and $Lu$ sensors. A correction was applied to the radiometric measurements through the instrument's calibration for the immersion effect (Satlantic MicroPro operation manual, 2002).

To estimate the water leaving radiance $Lw$, we extrapolated underwater $Lu(z)$ measurements to just below the water surface $z=0^{-}$ and estimated transmittance through the water-air interface. The upwelling radiance just below the water surface, $Lu(0^{-},\lambda)$ was estimated through non-linear least squares fitting (SigmaStat software) of measured $Lu(z,\lambda)$ to the equation $Lu(z,\lambda)= Lu(0^{-},\lambda)\ \exp(-K_{Lu}\cdot z)$, where $K_{Lu}$ is the diffuse attenuation coefficient for the upwelling radiance, to a good approximation constant in the layer 0-3 m used in the regressions. The coefficients of determination ($R^2$ values) for the non-linear exponential fits were in most cases

better than 0.99. To estimate $L$w, we calculated the propagation of $L$u(0$^-$,λ) through the water-air interface:

$$Lw(\lambda,\theta,\varphi) = Lu(0^-,\lambda,\theta',\varphi)\frac{(1-r(\theta',\theta))}{n_w^{\,2}} \qquad (2)$$

where $\theta'$ is the direction of the upward traveling photons incident from the water body onto the water surface, $\theta$ is the direction of the transmitted photons, $r(\theta',\theta)$ is the Fresnel reflectance for the associated directions $\theta'$ and $\theta$, and $n_w$ is the index of refraction of water ($n_w \approx 1.34$) (Mobley, 1994). For the geometry of our measurements, the zenith angle of water-leaving radiance and the nadir angle of in-water upward radiance are zero ($\theta'=\theta=0$) and the transmittance is $(1-r(\theta',\theta)) \approx 0.98$ (Mobley, 1994). Therefore, $L$w(λ) can be estimated from Eq. 2, as:

$$Lw(\lambda) = 0.544\ Lu(0^-,\lambda) \qquad (3)$$

Based on its definition, $R$rs(λ) was estimated as the ratio of the water-leaving radiance $L$w(λ) and measured surface downwelling irradiance $E$s(λ). Eq. 1 and measured $R$rs and IOPs ($a$ and $b_b$) were used to estimate variability in the quantity $f/Q$.

For those cases when in-situ measurements of $L$u profiles were not available we used the extensively validated Hydrolight underwater radiative transfer (RT) program (Mobley, 1988; 1994) to estimate $L$u(0$^-$), $L$w, and $R$rs for the bio-optical conditions observed in the Bay. Measured IOPs (i.e. $a$, $b$, $c$, $b_b$) and above-water $E$s were used as inputs to perform the model calculations. The Pope and Fry (1997) absorption values for pure water and the Smith and Baker (1981) seawater scattering coefficients with the Rayleigh-like pure-water scattering phase function were used in our RT simulations. Raman scattering, and CDOM and chlorophyll-a fluorescence were included in all model runs. Tzortziou et al. (submitted) discuss details of the methodology and results of RT model simulations using Hydrolight for the mid-mesohaline Chesapeake Bay, and the good RT optical closure they obtained.

*3.4. MODIS chlorophyll algorithms and products*

Three algorithms have been used with MODIS data for remote retrieval of chlorophyll concentrations:

i) The SeaWiFS-analog OC3M chlorophyll algorithm (currently operational MODIS level-2 standard chlorophyll product 'Chlor-a') is an empirical algorithm that relates the maximum of three blue-green *R*rs ratios to [chl-a] (O'Reilly et al., 2000; Eq. 4 in Table 3).

ii) The MODIS empirical-HPLC chlorophyll algorithm ('chlor_MODIS' product), is based on an empirical relationship derived from high performance liquid chromatography (HPLC) measurements of [chl-a] and blue-green *R*rs ratios measured in Case 1 and Case 2 waters (Clark, 1997; updated 19 Feb. 2002, D. Clark, personal communication) (Eq. 5 in Table 3). A recently proposed version of the algorithm (updated 19 March 2003, D. Clark, personal communication) is a $5^{th}$- order polynomial, expected to perform better in very high and very low chlorophyll environments.

iii) The MODIS semi-analytical chlorophyll algorithm ('chlor_a_3' product) is based on a bio-optical model that relates *R*rs to backscattering and absorption by phytoplankton and gelbstoff (combined term for CDOM and non-algal particles). Due to the similarity in the absorption spectral shapes of CDOM and non-algal particles the algorithm cannot separate contribution of each component to 'gelbstoff' absorption (Carder et al., 2002). The algorithm uses a semi-analytical approach in the sense that the relationship between *R*rs and water IOPs is based on radiative transfer theory and the approximate formula Eq. 1. However, for $a_{phyt}(675)$ larger than 0.03 $m^{-1}$, or [chl-a] higher than 1.5-2.0 mg $m^{-3}$, the MODIS semi-analytical algorithm automatically switches to an empirical relationship between [chl-a] and blue-green *R*rs ratios (Eq. 6 in Table 3).

In summary, when applied to waters with [chl-a] larger than ~2 mg $m^{-3}$, which is typically the case in coastal waters like Chesapeake Bay, all three MODIS algorithms are based on empirical relationships between [chl-a] and *R*rs ratios at blue-green wavelengths. To examine the performance of the MODIS algorithms in the mid-mesohaline Chesapeake Bay region we applied the satellite algorithms (Eq. 4, 5, and 6 in Table 3) to *R*rs spectra estimated based on our in-situ bio-optical data. We then compared these [chl-a] estimates to measured surface chlorophyll concentrations.

## 4. Results

### *4.1. Water optical characteristics and RT model simulations*

Water bio-optical characteristics showed large spatial and temporal variability during our measurements in the mid-mesohaline Chesapeake Bay. Relatively clear waters were observed during the fall cruises, with low biological activity and relatively low total absorption, total attenuation and chlorophyll concentration values. Higher chlorophyll concentrations, associated with large surface phytoplankton bloom events, were observed in spring and summer (Tzortziou, 2004). Surface [chl-a] values ranged from 3.5 mg $m^{-3}$ (station PI, 13 November 2001) to 74 mg $m^{-3}$ (station HB, 11 June 2001) with an average value of 14.7 mg $m^{-3}$ (Figure 2).

Measurements of absorption properties showed that non-covarying CDOM and non-algal particles in these Case 2 waters contribute considerably to light attenuation at the blue wavelengths used in the MODIS chlorophyll retrievals. Combined contribution by CDOM and non-algal particles to surface (0-1m) $a_{t\text{-}w}$ was on average 59% at 488 nm. Absorption by non-algal particles alone was on average 41% of $a_{t\text{-}w}$ at 488 nm, getting as large as 56% of $a_{t\text{-}w}(488)$ at the highly turbid station JT on 9 July 2001. Contribution by CDOM and non-algal particles to surface $a_{t\text{-}w}$ was even larger at shorter wavelengths (e.g. 73% at 412 nm) as a result of the exponential increase in the absorption of both substances with decreasing wavelength (Bricaud et al., 1981; Kishino et al., 1985). Estimated $S_{CDOM}$ had an average value of 0.018 $nm^{-1}$ with a standard deviation of 0.0032 $nm^{-1}$. $S_{nap}$ varied in a relatively narrower range compared to $S_{CDOM}$, and had an average value of 0.011 $nm^{-1}$ and a standard deviation of only 0.001 $nm^{-1}$.

Large spatial and temporal variation was observed in the magnitude of particulate backscattering in the Bay, with surface $b_b(530)$ ranging between 0.013 – 0.166 $m^{-1}$ (Tzortziou, 2004). Higher $b_b$ values were observed consistently at the near shore site JT, compared to the

other three stations. Estimated backscattering fraction values, $b_b/b$, ranged from 0.006 to 0.036 at 530 nm, with the largest $b_b/b$ value of 0.036 occurring close to the bottom at station JT. Average $b_b/b$ values, estimated as the average of measurements at all depths at the four stations, were 0.0133 (SD = 0.0032), 0.0128 (SD = 0.0032), and 0.0106 (SD = 0.0029), at 450, 530 and 650 nm, respectively. Surface $b_b/b$ at 530 nm, estimated from measurements within 1 m from the surface, had an average value of 0.0125 (SD = 0.003) at the four stations. Surface $b_b/b(530)$ was typically higher at the turbid station JT, with an average value of 0.0146 (SD = 0.0037).

Observed variability in water IOPs resulted in large spatial and temporal variability in the magnitude of measured *R*rs spectra (Tzortziou et al., 2004). However, in all cases, maximum values of *R*rs occurred at the green wavelengths because of the large pure-water absorption in the red, and the large CDOM and non-algal particulate absorption in the blue region of the spectrum.

*4.2. MODIS chlorophyll-a algorithm performance*

We examined the performance of the MODIS chlorophyll algorithms for the mid-mesohaline Chesapeake Bay by applying the MODIS algorithms to *R*rs spectra derived from our in-situ bio-optical data, and comparing estimated [chl-a] products to our in-situ measurements of surface chlorophyll concentrations. For the water conditions we observed in the mid-mesohaline Chesapeake Bay chlorophyll concentrations were consistently higher than 3.5 mg $m^{-3}$. For these [chl-a] values all MODIS chlorophyll retrievals are based on empirical relationships between [chl-a] and blue-green *R*rs ratios (Eq. 4-6, Table 3). Comparisons between estimated [chl-a] values with in-situ measured [chl-a] showed large disagreements for all satellite algorithms (Figure 3), although some of the algorithms were expected to perform better in high chlorophyll environments (e.g. $5^{th}$ order polynomial, "chlor_MODIS" product). Coefficients of determination

were in all cases between 0.3 and 0.35 (Table 4). These results were in agreement with the relatively weak correlation we observed between measured surface $\log_{10}$([chl-a]) and the *R*rs ratios used in the MODIS chlorophyll retrievals (i.e. $\log_{10}(Rrs(443)/Rrs(554))$ and $\log_{10}(Rrs(488)/Rrs(554))$. Coefficients of determination in the applied linear (and cubic) regressions were less than 0.39 (Table 4).

We then examined correlation between surface [chl-a] and various two-band *R*rs ratios using MODIS wavebands in the blue, green, and red wavelength regions (Table 4). The strongest correlation was found between [chl-a] and the ratio *R*rs(677)/*R*rs(554) ($R^2$=0.54). The empirical relationship found between [chl-a] and the red-green band ratio was consistent with expectations based on our in-situ bio-optical data (Tzortziou, 2004). Based on Eq. 1, and assuming $f/Q \cdot (t_{w\text{-}a} \cdot t_{a\text{-}w}) / n_w^2$ independent of wavelength and $b_b << a$ (Carder et al., 2002), the *R*rs ratio 677:554 is proportional to the backscattering ratio and inversely proportional to the absorption ratio at these two wavelengths (i.e. $Rrs(677)/Rrs(554) = b_b(677)/b_b(554) \cdot a(554)/a(677)$). For the mid-mesohaline Chesapeake Bay, $b_b$ in the green was strongly correlated with $b_b$ in the red ($R^2$=0.99; Table 4). Strong correlation and linear relationship ($R^2$=0.92) was also found between $a_{t\text{-}w}(554)$ and $a_{t\text{-}w}(677)$ based on our AC9 data (Table 4). As phytoplankton is the major absorber in the 677 nm wavelength region (other than pure water), absorption at 677 was expected to be strongly correlated with [chl-a], with some variation due to changes in phytoplankton species composition, physiological state, and size (Bricaud et al., 1995). Indeed, least squares regression for our data gave: $a_{t\text{-}w}(677) = 0.0166 \cdot$ [chl-a] + 0.0603 ($R^2$ = 0.92), with the small intercept due to the small, residual absorption by CDOM and non-algal particulate matter at 677 nm. Including the effect of chlorophyll fluorescence at 677 nm using detailed RT model simulations (Tzortziou, 2004), we found that the relationship observed between [chl-a] and *R*rs(677)/*R*rs(554) was

consistent with predictions based on independently derived relationships between [chl-a] and the ratio of water IOPs (i.e. $b_b$, $a$) at the two specific wavelengths.

*4.3. Observed variability in f/Q*

We examined the relationship between $R$rs(λ) and the ratio of water IOPs $\frac{b_b(\lambda)}{a(\lambda)+b_b(\lambda)}$ in the mid- mesohaline Chesapeake Bay using measured and model-estimated $R$rs spectra and in-situ data of surface $b_b(\lambda)$ and $a(\lambda)$ to: (i) examine the closure between independently measured inherent and apparent optical properties based on Eq. 1; (ii) assess variability in the quantity $f/Q$ (from the slope between $R$rs and $b_b/(a+b_b)$) for the nadir-viewing geometry of our measurements; and (iii) compare field results with RT model simulations for these Case 2 waters and previous theoretical studies on $f/Q$ variability for same viewing geometry but Case 1 waters (Morel and Mueller, 2002).

$R$rs values at 443, 532 and 670 nm were strongly correlated with $b_b/(a+b_b)$ at all three wavelengths, whether $R$rs was measured by the Satlantic MicroPro (Figure 4, solid circles) or calculated by Hydrolight when MicroPro was not available (Figure 4, open circles). Coefficients of determination ($R^2$ values) were larger than 0.9 in all cases. The linear least-square regression fits for $R\text{rs}_{\text{measured}}$ versus $b_b/(a+b_b)$ were very similar to the linear least-square regression fits for $R\text{rs}_{\text{model}}$ versus $b_b/(a+b_b)$, suggesting a good agreement between data and RT model simulations. $\frac{f}{Q}\cdot\frac{t_{(w,a)}t_{(a,w)}}{n_w^{\,2}}$, estimated as the slope coefficient in the linear least square regression of $R\text{rs}_{\text{measured}}$ or $R\text{rs}_{\text{model}}$ versus $b_b/(a+b_b)$ (Eq. 1), ranged from 0.0485 to 0.058 for different wavelengths with coefficients of variation in the estimated slopes less than 2.5%. Estimates of the quantity

$\frac{f}{Q}.\frac{t_{(w,a)}t_{(a,w)}}{n_w^{\,2}}$ derived as the ratio $R$rs : $b_b/(a+b_b)$ for each individual data set of $R$rs and IOPs had a standard deviation of less than 10% at all wavelengths, showing that the modeled $f/Q$ (i.e. slope in the regression $R$rs *vs* $b_b/(a+b_b)$) represented well the individual measurements over the whole range of conditions.

*4.4. Relationships between $b_b$, particulate matter, and Rrs*

To examine the effect of particulate backscattering on $R$rs variability for the mid-mesohaline Chesapeake Bay we applied simple linear regression to the $R$rs and $b_b$ values measured over the observed wide range of in-water optical characteristics (Figures 5(a)-(c)). Both measured and model estimated $R$rs values at 670 nm were strongly correlated with surface $b_b$ at 650 nm (Figure 5(c)) ($R^2$=0.88). The correlation between $R$rs and $b_b$ was statistically significant but not as strong at the shorter wavelengths (i.e. $R$rs(443) versus $b_b$(450) in Figure 5(a) with $R^2$=0.67, and $R$rs(532) versus $b_b$(530) in Figure 5(b) with $R^2$=0.77).

Variability in $R$rs(670) in these waters is mainly driven by changes in particulate backscattering because of the relatively large contribution by pure water to total absorption at 670 nm. Surface $b_b$ in the red ranged between 0.008 and 0.12 $m^{-1}$ during our measurements in the Bay. This variability in backscattering, by more than an order of magnitude, corresponds to more than an order of magnitude changes in $R$rs(670) (based on Eq. 1). $R$rs is also affected by changes in total in-water absorption. However, changes in dissolved and particulate absorption at 670 nm by an order of magnitude (i.e. $a_{t\text{-}w}(670)$ in the range 0.1-1 $m^{-1}$ for the mid-mesohaline Bay) are masked by the relatively large pure water absorption ($a_w(670)$= 0.44 $m^{-1}$; Pope and Fry, 1997) translating to changes in total absorption by less than a factor of 3. At shorter visible wavelengths, interference by pure water absorption is minimal. Therefore, $R$rs at 443 and 530 nm

are affected strongly by changes in both total absorption (strong contribution by non-covarying particulate and dissolved components) and total backscattering (contribution by suspended particles).

Surface particulate backscattering at all three wavelengths 440, 530 and 650 nm (only $b_b(650)$ nm shown in Figure 6) was strongly correlated with absorption by non-algal particles in the blue (e.g. 412 nm) and UV (e.g. 380 nm) where non-algal particulate absorption is particularly strong ($R^2 = 0.83$ for the linear least-square regression $b_b(650)$ *vs* $a_{nap}(380)$; Figure 6). The relationship between surface [chl-a] and surface $b_b$ was highly variable (Figure 7) and correlation was considerably smaller ($R^2=0.57$) compared to that between $b_b$ and $a_{nap}$.

Given the above results, a strong correlation would be expected between *R*rs(670) and magnitude of absorption by non-algal particles. Indeed, coefficients of determination for the linear least-squares regression between *R*rs(670) and surface $a_{nap}$ were 0.7 and 0.74 for absorption measurements at 412 and 380 nm, respectively (Figures 8(a)-(b), Table 4).

## 5. Discussion

Obtaining accurate information on the composition and concentration of dissolved and particulate, organic and inorganic matter in near shore waters using remotely sensed ocean color is critical for primary production studies, coastal water quality monitoring, and carbon cycling modeling. However, application of currently operational satellite algorithms in near shore waters like the Chesapeake Bay often results in erroneous retrievals, as shown here for the MODIS chlorophyll algorithms. In this paper we applied an extensive bio-optical dataset and detailed RT model results to examine the relative roles of different substances in light absorption and backscattering in the mid-mesohaline Chesapeake Bay, derive relationships between $R$rs and optical properties of individual water components, and evaluate methods for remote retrieval of surface [chl-a], $b_b$, and suspended particles in these optically complex Case 2 waters.

Effective remote retrieval of biogeochemical variables in coastal waters depends to a large extent on the accuracy of, and consistency among, the in-situ data used in the development, validation, and improvement of the applied remote sensing bio-optical algorithms. Thus, testing the degree of closure among bio-optical quantities independently measured in the field becomes critical for remote sensing applications. Before applying our bio-optical data to the interpretation of satellite ocean-color observations and the investigation of new bio-optical relationships for the Chesapeake Bay, we examined the consistency and degree of optical closure among our measurements using RT modeling (Tzortziou et al., 2004). Close agreement between data and model results over a wide range of conditions, with average absolute differences between modeled and measured $R$rs less than 10%, demonstrated very good optical closure between independently measured quantities. These results increased confidence in the accuracy of, and consistency among, our in-situ bio-optical data.

5.1. MODIS chlorophyll-a algorithm performance

Chlorophyll concentrations larger than 2 mg $m^{-3}$ are typically observed in the mid-mesohaline Chesapeake Bay (e.g. Magnuson et al., 2004). During our measurements, which covered a wide range of in-water conditions, measured [chl-a] was consistently larger than 3.5 mg $m^{-3}$. For such conditions ([chl-a]>2 mg $m^{-3}$) all MODIS chlorophyll retrievals are based on empirical relationships between [chl-a] and blue-green reflectance ratios (i.e. 443, 488 nm MODIS bands). When we applied these algorithms to measured *R*rs spectra to examine the MODIS algorithm performance in the mid-mesohaline Bay, we found large disagreement between estimated and measured surface [chl-a] (Figure 3). The weak performance of MODIS chlorophyll retrievals in these Case 2 waters is not surprising considering our results showing large contribution by non-covarying CDOM and non-algal particles to total light absorption in the blue. This large interference from CDOM and non-algal particulate absorption is not sufficiently accounted for in the MODIS algorithms. Our results are consistent with findings by Harding et al. (2005) who examined the performance of the SeaWiFS empirical chlorophyll algorithm OC4v4 in the Chesapeake Bay. The OC4v4 chlorophyll algorithm is the SeaWiFS "analog" of the currently default MODIS algorithm OC3M examined here. Wozniak and Stramski (2004) used Mie scattering calculations to show that even relatively low concentrations of mineral particles of the order of 0.1 g $m^{-3}$ can considerably affect chlorophyll estimations from standard SeaWiFS and MODIS algorithms that are based on blue-green reflectance ratios. In near-shore, estuarine waters like Chesapeake Bay, mineral particles concentrations are typically much larger (average concentration of 4.8 g $m^3$ measured during our cruises; unpublished data, G. Gallegos), strongly affecting the *R*rs signal in the blue-green.

Because of the strong interference from CDOM and non-algal particulate absorption in the blue-green, regionally-specific algorithms based on the strong chlorophyll-a fluorescence

signal in the near-infrared (NIR) or the chlorophyll-a absorption feature in the red (~ 675 nm) have been proposed for improved chlorophyll retrievals in highly turbid, coastal and inland waters (e.g. Gower et al., 1984; Gons, 1999; Ruddick et al., 2001). When we examined correlation between [chl-a] and various MODIS *R*rs ratios using our in-situ data for the mid-mesohaline Chesapeake Bay we found that variability in surface [chl-a] was most strongly correlated with changes in the ratio *R*rs(677)/*R*rs(554) (Table 4). The derived relationship between [chl-a] and *R*rs(677)/*R*rs(554) was consistent with predictions based on RT model simulations and observed relationships between in-situ data of [chl-a] and IOPs ($b_b$ and $a$) at the two specific wavelengths. In the 677 nm wavelength region phytoplankton absorption becomes relatively significant, due to the chl-a pigment absorption maximum at ~ 675 nm and the exponential decrease of both CDOM and non-algal particulate absorption with increasing wavelength. This, and the almost constant red-green ratio of backscattering coefficients measured in the mid-mesohaline Chesapeake Bay, suggest that most of the variability in the *R*rs ratio 677:554 is due to changes in [chl-a].

These results are first step towards the development of regionally-specific chlorophyll algorithms for the Chesapeake Bay using remotely sensed ocean reflectance in the red (i.e. ratio *R*rs(677)/*R*rs(554) for MODIS). Moreover, one of the main factors affecting the accuracy of satellite chlorophyll retrievals in near shore waters is correction for the atmosphere's optical characteristics. Problems with atmospheric correction of satellite data in the blue due to extrapolation of aerosol properties from NIR to shorter wavelengths (Gordon and Voss, 1999) are avoided when using the red wavelengths for chlorophyll retrievals. The relationships found here between [chl-a] and various *R*rs ratios for the Chesapeake Bay strongly suggest that exploiting the ocean color signal in the red-NIR, where interference from CDOM and non-algal particulate absorption is minimal, is necessary for improving satellite monitoring of biological activity in these Case 2 waters.

*5.2. Rrs, IOPs, and variability in f/Q*

Since *R*rs is related to the backscattering and absorption properties of all the optically active water constituents, approximate forms of Eq. 1 have commonly been used in the development of semi-analytical bio-optical models for remote retrieval of surface [chl-a] and IOPs in Case 2 waters. Such approximations are often based on the assumption that the quantity *f/Q* is independent of wavelength, or in-water and air-water boundary conditions (e.g. semi-analytic version of chlorophyll algorithm by Carder et al., 2002; Gordon et al., 1988). However, recent model results by Morel and Mueller (2002) for vertically homogeneous, Case 1 waters, suggest that variations in *f/Q* (due to its dependence on water IOPs and illumination conditions) are within the range 0.08 - 0.15. For nadir-viewing measurements of *R*rs, Morel and Mueller found that *f/Q* varies between 0.08 and 0.11 depending mainly on [chl-a], wavelength, and solar zenith angle (their figure 13.10).

Our detailed measurements of $b_b$, $a$, and *R*rs spectra allowed us to examine the relationship between *R*rs and the IOPs ratio $b_b/(a+b_b)$, and assess observed variability in the quantity *f/Q* for the nadir-viewing geometry of our measurements in the mid-mesohaline Chesapeake Bay. Close agreement in the resulting relationships between $b_b/(a+b_b)$ and *R*rs, whether *R*rs was measured in-situ or calculated by the RT model, demonstrated the consistency between our in-situ bio-optical dataset and RT model predictions for these Case 2 waters.

Estimated values of the quantity $\frac{f}{Q}.\frac{t_{(w,a)}t_{(a,w)}}{n_w^2}$, derived from the linear regression of $Rrs_{measured}$ versus $b_b/(a+b_b)$, ranged from 0.0485 to 0.058. These estimates were in good agreement with the $\frac{f}{Q}.\frac{t_{(w,a)}t_{(a,w)}}{n_w^2}$ values derived based on RT model simulations for the specific bio-optical

conditions observed in the Bay waters (i.e. slope of linear regression on $R\text{rs}_{\text{model}}$ versus $b_b/(a+b_b)$, Figure 4).

Since $t_{(a,w)}t_{(w,a)}/n_w^2$ is approximately equal to 0.54 (Mobley, 1994), our results regarding $\frac{f}{Q}.\frac{t_{(w,a)}t_{(a,w)}}{n_w^2}$ correspond to $f/Q$ values in the range 0.09 to 0.107. Interestingly, the range of $f/Q$ values we derived for the Case 2 Chesapeake Bay waters is very similar to the range of $f/Q$ values (0.08-0.11) reported by Morel and Mueller (2002) in their theoretical computations for same geometry of measurements (nadir-viewing), but Case 1 waters.

Our measurements in the Bay were performed over a wide range of water bio-optical characteristics (e.g. [chl-a] in the range 3.5 - 74 mg $m^{-3}$), at different solar zenith angles ($\theta_o$ between 16° and 58°), and for both hazy and clear atmospheric conditions. However, coefficients of variation in the estimated slopes of the linear regressions between $R$rs and $b_b/(a+b_b)$ (average $f/Q$ over a range of conditions) were less than 2.5%, and the standard deviation of the $f/Q$ values estimated from individual datasets of $R$rs and $b_b/(a+b_b)$ was less than 10%. These results, based on both in-situ data and RT model simulations, suggest that for the nadir viewing geometry of our measurements in these Case 2 waters, observed variability in the quantity $f/Q$ (and therefore in the ratio $R$rs : $b_b/(a+b_b)$) was not very large, and not considerably different from Case 1 waters.

*5.3. Rrs, $b_b$ processes, and particulate matter in the mid-mesohaline Chesapeake Bay*

As the spectral reflectance of the ocean is to a first approximation proportional to $b_b/(a+b_b)$, backscattering processes are of primary importance to applications of optical remote sensing in oceanography. Backscattering signal depends on the concentration, composition, size distribution, shape, and refractive index of suspended, organic and inorganic, marine particles

(van de Hulst, 1981). Thus, $b_b$ carries useful information about seawater constituents that affect biological activity, biogeochemical cycling, and carbon fluxes in coastal ecosystems. Carbon content in individual plankton cells has been found to be related to particle size (e.g. Verity et al., 1992; Montagnes et al., 1994) and refractive index (Stramski, 1999). Measurements by Stramski et al. (1999) in the Southern Ocean revealed high correlation between surface particulate backscattering at 510 nm and surface concentration of particulate organic carbon (POC). In coastal waters a significant fraction of suspended particulate matter consists of highly refractive, inorganic mineral particles, derived from coastal erosion, river discharge of terrigenous inorganic particles, bottom resuspension, or aeolian inputs (Stramski et al., 2004).

Particulate backscattering in the mid-mesohaline Chesapeake Bay showed large variation in magnitude, related to variations in particulate loading, mixing processes, and distance off-shore. Highly backscattering waters were observed near station JT, which is located closest to the land among the four sampling stations and is more strongly influenced by shoreline erosion and resuspension of bottom sediments due to tidal and land boundary effects (Figure 2). Variation in surface $b_b$ significantly affected *R*rs magnitude at all wavelengths (Figure 5), and was found to be the main factor driving observed variability in the *R*rs signal at 670 nm (Figure 5(c)). The strong correlation found between $b_b$ and *R*rs(670) indicates that satellite measured *R*rs at 670 nm can be applied to remotely retrieve particulate backscattering in these Case 2 waters.

Estimated backscattering fraction in the mid-mesohaline Chesapeake Bay had an average value of $\sim 0.013$ at 530 nm, in agreement with $b_b/b$ values reported by Sydor and Arnone, (1997) for the near shore waters off Mississippi. The observed spectral shape of $b_b/b$ is in agreement with Mobley et al. (2002) who measured a decrease in $b_b/b$ from 442 to 555 nm by less than 24 %, for the Case 2 waters offshore of New Jersey. Backscattering fraction can

provide a proxy to the particulate bulk refractive index, which in turn is an indicator of the particulate composition in the water (Twardowski et al., 2001; Sullivan et al., 2002, Stramski al., 2004). Due to their high water content phytoplankton cells have relatively low refractive index compared to inorganic particles (e.g. Carder et al., 1974; Aas, 1981; 1996; Stramski et al., 1988). As particulate backscattering increases with increasing particulate refractive index, $b_b/b$ values for phytoplankton-dominated waters are typically lower than those of waters where suspended inorganic particles and detrital material dominate (Twardowski et al., 2001; Sullivan et al., 2002). Measurements by Twardowski et al. (2001) in the Gulf of California and Boss et al. (2004) off the New Jersey coast showed that phytoplankton-dominated surface waters with high chlorophyll concentrations had $b_b/b$ values of ~0.005-0.006, while $b_b/b$ was higher (exceeding 0.012 according to Boss et al.) in regions where highly refractive re-suspended inorganic particles dominated. In agreement with these studies we observed the largest $b_b/b$ values ($b_b/b$ of 0.025-0.036) close to the bottom at station JT, consistent with an increase in the relative proportion of highly refractive re-suspended inorganic sediments in bottom waters. Surface $b_b/b(530)$ in the mid-mesohaline Bay had an average value of 0.0125. This is considerably larger than the $b_b/b$ values of 0.005-0.006 observed in surface coastal waters dominated by low refractive index phytoplankton particles (e.g. Twardowski et al., 2001; Boss et al., 2004). These results, and the even higher (average of 0.0146) surface $b_b/b$ measured at the highly turbid station JT, suggest that particulate backscattering in the mid-mesohaline Chesapeake Bay surface waters is dominated by suspended non-algal particles, such as highly refractive minerals or organic detritus with low water content (Twardowski et al., 2001; Green et al., 2003).

The inference of qualitative geochemical information on non-algal particles from their optical characteristics (e.g. absorption magnitude and $S_{nap}$) is still a major challenge for effective

remote sensing in coastal environments (e.g. Ferrari et al., 2003). The magnitude of non-algal particulate absorption in the mid-mesohaline Chesapeake Bay showed strong seasonal and temporal variability, and not strong covariation with CDOM or chlorophyll concentration (Tzortziou, 2004). However, there was little variation in the spectral shape of the non-algal particulate absorption, with $S_{nap}$ values within a narrow range around an average value of 0.011 $nm^{-1}$ (SD =0.001 $nm^{-1}$). Previous studies suggest that $S_{nap}$ values of about 0.011 are typical for mineral-dominated waters. Bowers et al. (1996) estimated an average $S_{nap}$ value of 0.010 (± 0.0002) for the absorption spectra of over 100 samples of mineral suspended solids collected from the Menai Strait in the Irish Sea. Measurements by Babin et al. 2003) at about 350 stations in European coastal waters showed that $S_{nap}$ had an average value of 0.0117 $nm^{-1}$ for the mineral-dominated waters in the North Sea and English Channel. Ferrari et al. (2003) measured $S_{nap}$ values in the range 0.0095 to 0.0125 for the coastal waters of the North Sea and German Bight where the main fraction of total suspended solids was inorganic (~ 76%). Relatively higher $S_{nap}$ values, in the range 0.0115 to 0.0145 were reported for the Baltic Sea, which is known for its high organic matter content (Voipo, 1981; Ferrari et al., 2003). Similarly, Babin et al. (2003) found that highly organic samples collected from the Baltic Sea were characterized by relatively higher, and statistically significantly different, $S_{nap}$ values compared to mineral-dominated waters, suggesting that observed variation in $S_{nap}$ may be related to the proportion of mineral and organic matter.

The large measured $b_b/b$ values relative to phytoplankton-dominated waters, and the close agreement between our estimates of $S_{nap}$ with $S_{nap}$ values reported in other studies for suspended inorganic particles, indicate a predominant backscattering role by highly-refractive non-algal particles with high inorganic content in the mid-mesohaline Chesapeake Bay.

Consistent with these results, we found that $b_b$, although highly variable, was strongly correlated with the magnitude of non-algal particulate absorption at 380 nm ($R^2$=0.83, Figure 6). These results, along with the small variability observed in $S_{nap}$, suggest that the high correlation between $a_{nap}$ and $b_b$ is caused by the dominance of the non-algal inorganic particle concentrations in controlling changes in both $a_{nap}$ and $b_b$ in these waters.

Our results of the high correlation between particulate $b_b$ and $a_{nap}$, in conjunction with remote retrieval of surface $b_b$ from *R*rs(670), suggest that *R*rs(670) can be applied to remotely determine abundance and distribution of non-algal particulate matter in near-shore regions where suspended inorganic particles strongly affect ocean color. For the mid-mesohaline Chesapeake Bay surface waters we showed that, indeed, *R*rs(670) is strongly correlated with the magnitude of non-algal particulate absorption at 380 nm (Figure 8). Binding et al. (2003) found good correlation between surface irradiance reflectance ($R = Eu/Ed$) at 665 nm and concentration of mineral suspended sediments for the Irish Sea waters. Due to the similarity in the absorption spectral shapes of CDOM and non-algal particles, separating contribution by the two components to total light absorption in Case 2 waters is a difficult task. As a result, most satellite Case 2 algorithms (e.g. Maritorena et al., 2002; Magnuson et al., 2004), including the MODIS semi-analytical chlorophyll algorithm (Carder et al., 2002), combine CDOM and non-algal particles to one term (e.g. "gelbstoff") even though the two components do not covary in coastal waters. Regional specific relationships, such as those we have derived here between $a_{nap}(380)$, $b_b(650)$, and *R*rs(670), separately estimate contribution by non-algal particulate matter to total light absorption based on the backscattering properties of the non-algal particles and the remote retrieval of particulate $b_b$ from satellite-measured *R*rs.

## 6. Summary and Conclusions

Effective interpretation of ocean color is a major challenge in near-shore Case 2 waters like the Chesapeake Bay. In order to deduce composition and concentration of water biogeochemical constituents from ocean color in these waters, it is imperative to apply accurate in-situ bio-optical data and RT model results to, first, evaluate the performance of currently operational satellite algorithms and, then, develop improved, and in most cases regionally-specific, retrieval methods. For the water conditions we observed in the Chesapeake Bay currently operational MODIS chlorophyll retrievals are based on empirical relationships between [chl-a] and blue-green *R*rs ratios. These algorithms cannot be expected to perform accurately in Case 2 waters where large concentrations of non-covarying CDOM and non-algal particles strongly affect the *R*rs signal in the blue. We found that relationships between [chl-a] and two-band *R*rs ratios in the long visible wavelengths (i.e. *R*rs(677)/*R*rs(554)), where interference from CDOM and non-algal particulate absorption is minimal, provide a better basis for satellite monitoring of phytoplankton blooms in the mid-mesohaline Bay. Our measured $b_b/b$ and $S_{nap}$ values indicated a dominant role by highly-refractive non-algal particles in regulating backscattering variability in these waters, which was consistent with the strong correlation found between $a_{nap}$ and particulate $b_b$. Relating these results to ocean color data, we found that $b_b$ is the main factor driving observed variability in *R*rs(670), a quantity that can be measured remotely. Retrieval of particulate $b_b$ from satellite measured *R*rs(670) can be applied to remotely monitor distribution and concentrations of highly refractive suspended particles in the mid-mesohaline Chesapeake Bay. Moreover, retrieval of non-algal particulate absorption from the reflectance signal at 670 nm could be used in conjunction with inversion of UV-blue wavelengths to derive CDOM absorption in these Case 2 waters. Separating contribution by these two similarly

absorbing, but non-covarying, components to total light absorption is particularly useful for remote sensing of CDOM and studies on dissolved organic carbon cycling in coastal waters. Very good optical closure results, achieved using detailed RT modeling, increased confidence on the accuracy of, and consistency among the data presented in this study. Quantitative analysis of particulate composition, and measurements of the differences in the optical characteristics (i.e. $S_{nap}$ and $b_b$) between organic detrital and inorganic mineral suspended particles are needed to improve interpretation of remote sensing in coastal regions like Chesapeake Bay where non-algal particles often dominate the backscattered signal.

**Acknowledgements**

Funds for this work were provided by NASA-Goddard Space Flight Center, the University of Maryland, and the Smithsonian Institution Fellowship program. Field work in Chesapeake Bay was funded in part by the Coastal Intensive Site Network (CISNet) program of the United States Environmental Protection Agency through grant R826943-01-0. We thank K. Yee, D. Sparks, M. Mallonee and S. Benson for assistance in the field and laboratory.

**References**

Aas, E., 1981, The refractive index of phytoplankton, Rep. 46, 61 pp., Inst. Geophys., Univ. of Oslo, Oslo, Norway

Aas, E., 1996, Refractive index of phytoplankton derived from its metabolite composition, *Journal of Plankton Research*, 18, 2223–2249.

Austin, R.W., 1974, The remote sensing of spectral radiance from below the ocean surface. In: *Optical Aspects of Oceanography. N.G. Jerlov and E. Steemann-Nielsen (Eds.),* Academic Press, London, New York, 317-344.

Babin M., Stramski D., Ferrari G., Clauster H., Bricaud A., Obelensky G., and Hoepffner N., 2003, Variations in the light absorption coefficients of phytoplankton, nonalgal particles, and dissolved organic matter in coastal waters around Europe, *Journal of Geophysical Research*, Vol. 108, N. C7, 3211

Binding C. E., Bowers D.G., and Mitchelson-Jacob E.G., 2003, An algorithm for the retrieval of suspended sediment concentrations in the Irish Sea from SeaWiFS ocean colour satellite imagery, *International Journal of Remote Sensing*, Vol. 24, No 19, 3791–3806

Blough, N.V. and Del Vecchio R., 2002, Chromophoric Dissolved Organic Matter (CDOM) in the Coastal Environment. In: *Biogeochemistry of Marine Dissolved Organic Matter* (D.A. Hansell and C.A. Carlson, Eds.), Academic Press, 509-546

Boss E., Pegau W. S., Lee M., Twardowski M. S., Shybanov E., Korotaev G., and Baratange F., 2004, The particulate backscattering ratio at LEO 15 and its use to study particles composition and distribution. *Journal of Geophysical Research*, 109, C01014, doi:10.1029/2002JC001514

Bowers, D. G., Harker G. E. L., and Stephan B., 1996, Absorption spectra of inorganic particles in the Irish Sea and their relevance to remote sensing of chlorophyll, *International Journal of Remote Sensing*, 17(12), 2449–2460

Bricaud, A., Babin, M., Morel, A. and Claustre, H., 1995, Variability in the chlorophyll-specific absorption coefficients of natural phytoplankton : analysis and parameterization. *Journal of Geophysical Research,* 100(C7): 13,321-13,332.

Bricaud, A., Morel, A. and Prieur, L., 1981, Absorption by dissolved organic matter of the sea (yellow substance) in the UV and visible domains. *Limnology and Oceanography,* 26(a): 43-53.

Carder K. L., Betzer P. R., and Eggimann D. W., 1974, Physical, chemical, and optical measures of suspended particle concentrations: Their intercomparison and application to the west African shelf, in *Suspended Solids in Water*, edited by R. J. Gibbs, pp. 173–193, Plenum, New York

Carder K. L., Chen F. R., Cannizzaro J. P., Campbell J. W. and Mitchell B. G., 2004, Performance of the MODIS semi-analytical ocean color algorithm for chlorophyll-a, *Advances in Space Research* 33: (7) 1152-1159

Carder, K. L., Chen R. F., and Cannizzaro J.P., 2002, "Case 2 Chlorophyll a" MODIS Ocean Science Team Algorithm Theoretical Basis Document, ATBD 19, Version 6

Carder, K.L., Hawes S.K., Baker K.A., Smith R.C., Steward R.G., and Mitchell B.G., 1991, Reflectance model for quantifying chlorophyll a in the presence of productivity degradation products, *Journal of Geophysical Research*, 96, 20,599–20,611

Clark D. K., 1997, Bio-Optical Algorithms Case 1 Waters, MODIS Algorithm Theoretical Basis Document

Darecki M., and Stramski D., 2004, An evaluation of MODIS and SeaWiFS bio-optical algorithms in the Baltic Sea, *Remote Sensing of Environment* 89: (3) 326-350

Ferrari G. M., Bo F. G., Babin M., 2003, Geo-chemical and optical characterizations of suspended matter in European coastal waters, *Estuarine, Coastal and Shelf Science* 57, 17–24

Gallegos C. L. and Neale P. J., 2002, Partitioning spectral absorption in case 2 waters: Discrimination of dissolved and particulate components, *Applied Optics*, 41, 4220-4233

Garver S. A, and Siegel D. A., 1997, Inherent optical property inversion of ocean color spectra and its biogeochemical interpretation. I. Time series from the Sargasso Sea, *Journal of Geophysical Research*, 102, 18607–18625

Glibert, P.M., D.J. Conley, T.R. Fisher, L.W. Harding, and T.C. Malone, 1995, Dynamics of the 1990 winter/spring bloom in Chesapeake Bay, *Marine Ecology Progress Series*, 122:22-43.

Gons H. J., 1999, Optical teledetection of chlorophyll *a* in turbid inland waters," Environ. Sci. Technol. 33, 1127–1133

Gordon H. R, Brown O. B., Evans R. H., Brown J. W., Smith R. C., Baker K. S., and Clark D. K., 1988, A semi-analytic model of ocean color, *Journal of Geophysical Research*, 93, 10,909–10,924

Gordon H.R., and Ding K., 1992, Self-shading of in-water optical instruments, *Limnology and Oceanography*, 37, 491-500

Gordon, H. R., Brown O. B., and Jacobs M. M., 1975, Computed relationships between the inherent and apparent optical properties of a flat homogeneous ocean, *Applied Optics*, 14, 417–427.

Gordon, H. R. and Voss K. J., 1999, MODIS Normalized Water-leaving Radiance, Algorithm Theoretical Basis Document, Version 4, MOD 18.

Gower J. F. R., Lin S., and Borstad G. A., 1984, The information content of different optical spectral ranges for remote chlorophyll estimation in coastal waters, *International Journal of Remote Sensing*, 5, 349–364

Green R. E., Sosik H. M., and Olson R. J., 2003, Contributions of phytoplankton and other particles to inherent optical properties in New England continental shelf waters, *Limnology and Oceanography*, 48(6), 2377–2391

Gregg, W.W., and Conkright, M.E., 2001, Global Seasonal Climatologies of Ocean Chlorophyll: Blending In situ and Satellite Data for the CZCS Era, *Journal of Geophysical Research*, 106: 2499-2515.

Harding Jr. L.W., Magnuson A., Mallonee M.E., 2005, Bio-optical and remote sensing observations in Chesapeake Bay, *Estuarine, Coastal and Shelf Science*, 62, 75-94

Harding L. W., and Magnuson A., 2002, Bio-Optical and Remote Sensing Observations in Chesapeake Bay, in *SIMBIOS Project 2001 Annual Report*, G. S. Fargion and C. R. McClain, eds. (NASA/TM, 2002), 52-62.

Harding L. W., Itsweire E. C., and Esaias W. E., 1992, Determination of Phytoplankton Chlorophyll Concentrations in the Chesapeake Bay with Aircraft Remote Sensing, *Remote Sensing of the Environment*, 40, 79-100.

Harding, L. W., and Perry, E. 1997, Long-term increase of phytoplankton biomass in Chesapeake Bay, 1950–94, *Marine Ecology Progress Series*, 157, 39–52.

Hoge F. E., and Swift R. N., 1981, Application of the NASA Airborne Oceanographic Lidar to the mapping of chlorophyll and other organic pigments, in Chesapeake Bay Plume Study – Superflux 1980 (J. W. Campbell and J. P. Thomas, Eds.) NASA Conf. Publ. 2188, NOAA/NEMP III 81 ABCDFG 0042

Jeffrey S. W., and Humphrey G. F., 1975, New spectrophotometric equations for determining chlorophyll a, b, c, and c2 in higher plants algae and natural phytoplankton, *Biochemie and Physiologie der Pflanzen*, 167, 191-194

Johnson D. R., Weidemann A., Arnone R., Davis C.O., 2001, Chesapeake Bay outflow plume and coastal upwelling events: Physical and optical properties, *Journal of Geophysical Research*, Vol 106, No C6, 11,613–11,622

Kemp W. M., and Boynton W. B., 1992, Benthic-pelagic interactions: Nutrient and oxygen dynamics, p. 149-221. In D. E.Smith, M. Leffler, and G. Mackiernan (eds.), Oxygen Dynamics in the Chesapeake Bay: A Synthesis of Research. Maryland Sea Grant College, College Park, Maryland.

Kirk, J. T. O., 1984, Dependence of relationship between inherent and apparent optical properties of water on solar altitude, *Limnology and Oceanography*, 29, 350–356.

Kirk, J. T. O., 1992, Monte Carlo modeling of the performance of the reflective tube absorption meter, *Applied Optics*, 31, 6463-6468

Kishino, M., Takahashi, M., Okami, N. and Ichimura, S., 1985, Estimation of the spectral absorption coefficients of phytoplankton in the sea. *Bulletin of Marine Science,* 37: 634-642.

Lee, Z. P., Carder K. L., Hawes S. H., Steward R. G., Peacock T. G., and Davis C.O., 1994, A model for interpretation of hyperspectral remote-sensing reflectance, *Applied Optics*, 33, 5721–5732.

Lobitz, B., Johnson L., Mountford K., and Stokely P., 1998, AVIRIS analysis of water quality in the Chesapeake Bay, Proceedings Fifth Int'l Conference Remote Sensing for Marine and Coastal Environments, vol. 1, 5-7 October, San Diego CA.

Longhurst A., Sathyendranath S., Platt T., and Caverhill C., 1995, An estimate of global primary production in the ocean from satellite radiometer data, *Journal of Plankton Research*, 17, 1245-1271

Maffione, R. A., and Dana D. R., 1997, Instruments and methods for measuring the backward-scattering coefficient of ocean waters, *Applied Optics*, 36, 6057– 6067

Magnuson A., Harding L. W., Mallonee M. E., Adolf J. E., 2004, Bio-optical model for Chesapeake Bay and the middle Atlantic bight, *Estuarine, Coastal and Shelf Science,* 61, 403-424

Malone, T. C., 1992, Effects of water column processes on dissolved oxygen: nutrients, phytoplankton and zooplankton, In Oxygen Dynamics in Chesapeake Bay: A Synthesis of Research (Smith, D., Leer, M. & Mackiernan, G., eds). University of Maryland Sea Grant, College Park, MD, 61–112.

Maritorena S., Siegel D. A., and Peterson A. R., 2002, Optimization of a semianalytical ocean color model for global-scale applications, *Applied Optics*, 41

McClain, C.R., Feldman, G.C. and Hooker, S.B., 2004, An overview of the SeaWiFS project and strategies for producing a climate research quality global ocean bio-optical time series, *Deep Sea Research. II. Topical Studies in Oceanography* 51: 5-42

Mitchell G., Bricaud A., Carder K., Cleveland J., Ferrari G., Gould R., Kahru M., Kishino M., Maske H., Moisan T., Moore L., Nelson N., Phinney D., Reynolds R., Sossik H., Stramski D., Tassan S., Trees C. C., Weidemann A., Wieland J., and Vodacek A., 2000, Determination of spectral absorption coefficients of particles, dissolved material and phytoplankton for discrete water samples, in *Ocean Optics Protocols For Satellite Ocean Color Sensor Validation*, Revision 2, G. S. Fargion and J. L. Mueller, NASA/TM-2000-209966, Chapter 12

Mobley C. D., 1988, A numerical model for the computation of radiance distribution in natural waters with wind-roughened surfaces, part II; user's guide and code listing, NOAA Tech. Memo ERL PMEL-81 (NTIS PB88-246871) (Pacific Marine Environmental Laboratory, Seattle, Wash.).

Mobley C. D., 1994, *Light and Water: Radiative Transfer in Natural Waters* (Academic Press, San Diego, Calif)

Mobley C. D., Sundman L. K., and Boss E., 2002, Phase function effects on oceanic light fields, *Applied Optics*, 41, 1035-1050.

Montagnes, D. J., Berges, J. A., Harrison, P. J., and Taylor, F. J. R., 1994, Estimation of carbon, nitrogen, protein, and chlorophyll a from volume in marine phytoplankton. *Limnology and Oceanography*, 39, 1044-1060

Moore, C., Twardowski M.S., and Zaneveld J.R.V., 2000, The ECO VSF – A multi-angle scattering sensor for determination of the volume scattering function in the backward direction. Proceedings from Ocean Optics XV, October 16-20, Monaco

Morel A., and Gentili B., 1991, Diffuse reflectance of oceanic waters: its dependence on Sun angle as influenced by the molecular scattering contribution", *Applied Optics*, 30, 4427-4438.

Morel A., and Gentili B., 1993, Diffuse reflectance of oceanic waters. II. Bidirectional aspects, *Applied Optics*, 32, 6864-6879.

Morel A., and Mueller J. L., 2002, Normalized water-leaving radiance and remote sensing reflectance: Bidirectional reflectance and other factors, *Ocean Optics Protocols for satellite ocean color sensor validation*, Chapter 13

Morel A., and Prieur L., 1977, Analysis of variations in ocean color, *Limnology and Oceanography*, 22, 709-722.

Morel A., Antoine D., and Gentili B., 2002, Bidirectional reflectance of oceanic waters: Accounting for Raman emission and varying particle scattering phase function, *Applied Optics* 41: 6289–6306, 247.

O'Reilly, J.E., Maritorena, S., Siegel, D., O'Brien, M.C., Toole, D., Mitchell, B.G., Kahru, M., Chavez, F.P., Strutton, P., Cota, G., Hooker, S. B., McClain, C.R., Carder, K.L., Muller-Karger, F., Harding, L., Magnuson, A., Phinney, D., Moore, G.F., Aiken, J., Arrigo, K.R., Letelier, R., and Culver, M., 2000, Ocean color chlorophyll a algorithms for SeaWiFS, OC2, and OC4: Version 4. *In: SeaWiFS Postlaunch Technical Report Series, edited by Hooker, S.B and Firestone, E.R. Volume 11, SeaWiFS Postlaunch Calibration and Validation Analyses, Part 3. NASA, Goddard Space Flight Center, Greenbelt, Maryland.* 9-23.

Pegau, W. S., Gray, D., Zaneveld, J. R. V., 1997, Absorption and attenuation of visible and near-infrared light in water: dependence on temperature and salinity. *Applied Optics* 36, 6035 - 6046.

Pope R. M., and Fry E. S., 1997, Absorption spectrum (380-700 nm) of pure water. II. Integrating measurements, *Applied Optics*, 36, 8710-8723.

Preisendorfer R. W., 1976, *Hydrological Optics* (6 volumes) (U.S. Dept. of Comm., NOAA, Honolulu, HA).

Ruddick K. G., Gons H.J., Rijkeboer M., and Tilstone G., 2001, Optical remote sensing of chlorophyll *a* in case 2 waters by use of an adaptive two-band algorithm with optimal error properties, *Applied Optics*, Vol. 40, No. 21, 3575-3585

Satlantic, 2000, Operation Manual for the MicroPro, Revision D, June 2002

Smith R. C., and Baker K. S., 1981, Optical properties of the clearest natural waters (200-800 nm), *Applied Optics*, 20, 177-184.

Stramski, D., 1999, Refractive index of planktonic cells as a measure of cellular carbon and chlorophyll a content, *Deep-Sea Research Part I*, 46, 335–351

Stramski, D., Boss E., Bogucki D., and Voss K. J., 2004, The role of seawater constituents in light backscattering in the ocean, *Progress in Oceanography*, 61(1), 27-55

Stramski, D., Morel A., and Bricaud A., 1988, Modeling the light attenuation and scattering by spherical phytoplankton cells: A retrieval of the bulk refractive index, *Applied Optics*, 27, 3954–3956

Stramski, D., Reynolds R.A., Kahru M., and Mitchell B.G., 1999, Estimation of particulate organic carbon in the ocean from satellite remote sensing, *Science*, 285(5433), 239–242.

Sullivan, J.M., Twardowski M.S., Donaghay P.L., and Freeman S., 2002, Particulate bulk refractive index distributions in coastal regions as determined from backscattering ratio measurements. Proceedings from Ocean Optics XVI, November 18–22, Santa Fe.

Sydor, M., Arnone, R.A., 1997, Effect of suspended particulate and dissolved organic matter on remote sensing of coastal and riverine waters, *Applied Optics 36,* 6905–6912.

Twardowski M., Boss E., Macdonald J. B., Pegau W. S., Barnard A. H., and Zaneveld J. R. V., 2001, A model for estimating bulk refractive index from the optical backscattering ratio and the implications for understanding particle composition in case I and case II waters, *Journal of Geophysical Research*, 106, 14,129-14,142.

Tzortziou M., 2004, Measurements and characterization of optical properties in the Chesapeake Bay's estuarine waters, using in-situ measurements, MODIS satellite observations and radiative transfer modelling, PhD-Dissertation, Dept of Meteorology, Univ. of Maryland, College Park, MD.

Tzortziou M., Herman J., Subramaniam A., Neale P., Gallegos C., Harding L., 2004, A closure experiment for in-water optical properties and radiation in the Chesapeake Bay estuarine waters, Abstract ASLO/TOS Ocean Research 2004 Conference, Honolulu, HI, February 15-20

Tzortziou M., Herman J., Gallegos C., Neale P., Subramaniam A., Harding L., Ahmad Z., submitted to Estuarine, Coastal, and Shelf Science, Bio-Optics of the Chesapeake Bay from Measurements and Radiative Transfer Calculations

van de Hulst, H. C., 1981, *Light Scattering by Small Particles*, 470 pp., Dover, Mineola, N. Y.

Verity P. G., Robertson C. Y., Tronzo C. R., Andrews M. G., Nelson J. R., and Sieracki M. E., 1992, Relationships between cell volume and the carbon and nitrogen content of marine photosynthetic nanoplankton, *Limnology and Oceanography*, 37, 1434–1446.

Voipo, A., 1981, The Baltic Sea, 416 pp., Elsevier Science, New York

Voss K.J., 1989, Use of the radiance distribution to measure the optical absorption coefficient in the ocean, *Limnology and Oceanography*, 34:1614–1622.

Voss K.J., and Morel A., 2005, Bidirectional reflectance function for oceanic waters with varying chlorophyll concentrations: Measurements versus predictions, *Limnology and Oceanography*, 50(2), 698–705

Wozniak S.B. and Stramski D, 2004, Modeling the optical properties of mineral particles suspended in seawater and their influence on ocean reflectance and chlorophyll estimation from remote sensing algorithms, Applied Optics, Vol. 43, No. 17

Yentsch, C.S., 1993, CZCS: Its role in the study of the growth of oceanic phytoplankton. In: Ocean Colour: Theory and Applications in a Decade of CZCS Experience, V. Barale and P. M. Schlittenhardt (eds.), Kluwer Academic Publishers, Dordrecht, The Netherlands, 17-32.

Yoder, J.A. and Kennelly M. A., 2003, Seasonal and ENSO variability in global ocean phytoplankton chlorophyll derived from 4 years of SeaWiFS measurements, *Global Biogeochemical Cycles* 17: (4)

Zibordi G. and Ferrari G. M., 1995, Instrument self-shading in underwater optical measurements: experimental data, *Applied Optics*, 34, 2750-2754

**Figure Legends:**

**Figure 1:** Location of in-situ measurements (stations HB, PI, TI and JT) and cruise track. The starting point during our cruises was the SERC dock located in the Rhode River sub-estuary, along the western shore of the Chesapeake Bay.

**Figure 2:** Frequency histogram of measured surface [chl-a].

**Figure 3:** Comparisons between measured [chl-a] and chlorophyll concentrations derived from the MODIS empirical algorithms using our field data and estimates of *R*rs and *nL*w spectra as input to the algorithms (chlorophyll values in logarithmic scales; N=40). The MODIS chl-

algorithms used were: (a) "Chlor_a" (Eq. 4); 'chlor_a_3' (Eq. 6) (b) for the 'unpackaged', and (c) for the 'fully packaged' cases; (d) 'chlor MODIS' (Eq. 5) for the high chl-a pigment (always the case in mid- and upper-Chesapeake Bay); (e) 'chlor MODIS', 5th order polynomial (D. Clark, updated 19 March 2003)).

**Figure 4:** Relation between measured *R*rs(λ) values and measured $\frac{b_b(\lambda)}{a(\lambda)+b_b(\lambda)}$ (solid circles), and between model-estimated *R*rs(λ) values and measured $\frac{b_b(\lambda)}{a(\lambda)+b_b(\lambda)}$ (open circles) at (a) 440 nm, (b) 530 nm and (c) 670 nm. Linear least-squares regression fits are shown as solid lines for $Rrs_{measured}$ and dashed lines for $Rrs_{model}$ ($R^2$ between 0.90-0.98; P<0.0001 in all cases). Regression results are summarized in Table 4.

**Figure 5:** Relation between measured $b_b$ and measured *R*rs (solid circles), and between measured $b_b$ and model-estimated *R*rs (open circles) at wavelengths (a) 443 nm ($b_b$ measured at 450 nm), (b) 532 nm ($b_b$ measured at 530 nm) and (c) 670 nm ($b_b$ measured at 650 nm) ($R^2$ are given in Table 4).

**Figure 6:** Relation between surface measurements of $b_b(650)$ and $a_{nap}$ at (a) 380 nm ($R^2$=0.83, N=43, P<0.0001) and (b) 412 nm ($R^2$=0.76, N=43, P<0.0001).

**Figure 7:** Relation between surface [chl-a] and surface $b_b(650)$ measurements in the Chesapeake Bay waters ($R^2$ are given in Table 4).

**Figure 8:** Linear regression between measured or model-estimated (based on measured IOPs) *R*rs values at 670 nm and surface measurements of absorption by non-algal particles at (a) 380 nm and (b) 412 nm (N=33, P<0.0001) ($R^2$ are given in Table 4).

**Table 1:** Dates of cruises in the Bay, and instrumentation for measurements of radiation fields. The AC9 and ECOVSF3 instruments were used in all cruises for measurements of water IOPs

| **Date of cruise** | **Instrument used for radiation fields** |
|---|---|
| 2001, June 4 | Satlantic OCI-200 |
| 2001, June 11 | Satlantic OCI-200 |
| 2001, June 25 | Satlantic OCI-200 |
| 2001, July 9 | Satlantic OCI-200 |
| 2001, September 21 | Satlantic SMSR |
| 2001, September 26 | Satlantic MicroPro |
| 2001, September 28 | Satlantic MicroPro |
| 2001, October 4 | Satlantic OCI-200 |
| 2001, October 30 | Satlantic MicroPro |
| 2001, November 13 | Satlantic OCI-200 |
| 2002, May 6 | Satlantic MicroPro |
| 2002, May 15 | Satlantic MicroPro |
| 2002, May 22 | Satlantic MicroPro |
| 2002, June 6 | Satlantic OCI-200 |
| 2002, June 18 | Satlantic OCI-200 |
| 2002, June 28 | - |
| 2002, November 8 | Satlantic MicroPro |

**Table 2:** In situ measurements of IOPs and radiation fields in the Chesapeake Bay.

| Measured quantities | Wavelength-range (in nm) | Instrument Used |
|---|---|---|
| Total absorption (minus absorption by pure water), $a_{t\text{-}w}$ | 412, 440, 488, 510, 532, 554, 650, 676, 715 | AC-9 |
| Total attenuation (minus attenuation by pure water), $c_{t\text{-}w}$ | 412, 440, 488, 510, 532, 554, 650, 676, 715 | AC-9 |
| Total backscattering, $b_b$ | 450, 530, 650 | ECO-VSF |
| Chlorophyll-a concentration, [chl-a] | | Spectrophotometric measurements |
| Phytoplankton absorption, $a_{phyt}$ | 290 – 750 | CARY-IV spectrophotometer |
| Non-algal particulate absorption, $a_{nap}$ | 290 – 750 | CARY-IV spectrophotometer |
| CDOM absorption, $a_{CDOM}$ | 290 – 750 | CARY-IV spectrophotometer |
| In-water Upwelling radiance profiles, *L*u | 400, 412, 443, 455, 490, 510, 532, 554, 564, 590, 625, 670, 684, 700 | Satlantic, MicroPro |
| In-water Downwelling irradiance profiles, *E*d | 400, 412, 443, 455, 490, 510, 532, 554, 564, 590, 625, 670, 684, 700 | Satlantic, MicroPro |
| In-water Upwelling irradiance profiles, *E*u | 412, 443, 490, 510, 554, 665, 684 | Satlantic, OCI-200 |
| In-water Downwelling irradiance profiles, *E*d | 325, 340, 380, 412, 443, 490, 510, 532, 554, 620, 665, 684, 706 | Satlantic, OCI-200 |
| Above-water Surface Downwelling Irradiance, *E*s | 400, 412, 443, 455, 490, 510, 532, 554, 564, 590, 625, 670, 684, 700 | Satlantic OCR-507 Irradiance Sensors |

**Table 3:** Summary of MODIS empirical chl-a algorithms

| MODIS empirical chl-a algorithms | Parameters |
|---|---|
| **MODIS OC3M, "Chlor_a" product:**<br><br>$\log_{10}[\text{chl-a}] = A + B \cdot R_{3M} + C \cdot R_{3M}^2 + D \cdot R_{3M}^3 + E \cdot R_{3M}^4$ (Eq 4) | $R_{3M} = \log_{10}(\max[\frac{Rrs(443)}{Rrs(551)}, \frac{Rrs(488)}{Rrs(551)}])$<br>A=0.283<br>B=-2.753<br>C=1.457<br>D=0.659<br>E=-1.403 |
| **MODIS empirical-HPLC, "chlor_MODIS" product:**<br>$\log_{10}[\text{chl-a}]=[A(\log_{10}(X))^3+ B(\log_{10}(X))^2+C(\log_{10}(X))^1+D]/E$ (Eq 5)<br>Different sets of A-E parameters are used for waters with high and low [chl-a]. *nL*w is the normalized water leaving radiance (Gordon and Clark; 1981), which can be estimated by multiplying *R*rs(λ) with the extraterrestrial solar irradiance, *F*o(λ)). | $X = \frac{nLw(443) + nLw(488)}{nLw(551)}$<br>High Chl-a pigm: A=-2.8237, B=4.7122, C=-3.9110, D=0.8904, E=1.0<br>Low Chl-a pigm.: A=-8.1067, B=12.0707, C=-6.0171, D=0.8791, E=1.0 |
| **Carder et al (2002), "chlor_a_3" product:**<br>$\log_{10}[\text{chl-a}]= c_o+ c_1\log_{10}(X)+c_2(\log_{10}(X))^2+c_3(\log_{10}(X))^3$ (Eq 6)<br>Parameters $c_o$ - $c_3$ are adjusted dynamically (based on information on the sea surface temperature) in order to account for pigment packaging effects ('packaged', 'un-packaged', and transitional cases) in nutrient-replete and nutrient-deplete conditions. | $X = \frac{Rrs(488)}{Rrs(551)}$<br>Unpackaged: $c_o = 0.2818$, $c_1 = -2.783$, $c_2 = 1.863$, $c_3 = -2.387$<br>Fully Packaged: $c_o = 0.51$, $c_1 = -2.34$, $c_2 = 0.4$, $c_3 = 0.0$ |

**Table 4:** Regression Relationships between IOPs and *R*rs in the mid-mesohaline Chesapeake Bay

| **Parameters (Y *vs* X)** | **Regression Relationship** | **$R^2$** |
|---|---|---|
| *R*rs(412)/*R*rs(554) *vs* $[\text{chl-a}]_{\text{in-situ}}$ | $\log_{10}(Y) = -0.354 \cdot \log_{10}(X) - 0.4508$ | 0.24 |
| *R*rs(443)/*R*rs(554) *vs* $[\text{chl-a}]_{\text{in-situ}}$ | $\log_{10}(Y) = -0.1537 \cdot \log_{10}(X) - 0.2933$ | 0.39 |
| *R*rs(488)/*R*rs(554) *vs* $[\text{chl-a}]_{\text{in-situ}}$ | $\log_{10}(Y) = -0.1299 \cdot \log_{10}(X) - 0.1074$ | 0.32 |
| *R*rs(510)/Rrs(554) *vs* $[\text{chl-a}]_{\text{in-situ}}$ | $\log_{10}(Y) = -0.1168 \cdot \log_{10}(X) - 0.0339$ | 0.36 |
| *R*rs(532)/*R*rs(554) *vs* $[\text{chl-a}]_{\text{in-situ}}$ | $\log_{10}(Y) = -0.0728 \cdot \log_{10}(X) + 0.0068$ | 0.23 |
| *R*rs(670)/*R*rs(554) *vs* $[\text{chl-a}]_{\text{in-situ}}$ | $\log_{10}(Y) = 0.166 \cdot \log_{10}(X) - 0.5467$ | 0.48 |
| *R*rs(677)/*R*rs(554) *vs* $[\text{chl-a}]_{\text{in-situ}}$ | $\log_{10}(Y) = 0.1725 \cdot \log_{10}(X) - 0.5117$ | 0.54 |
| $a_{t\text{-}w}(677)$ *vs* $[\text{chl-a}]_{\text{in-situ}}$ | $Y = 0.0166 \cdot X + 0.0603$ | 0.92 |
| $a_{t\text{-}w}(554)$ *vs* $a_{t\text{-}w}(677)$ | $Y = 0.68 \cdot X + 0.08$ | 0.92 |
| $b_b(650)$ vs $b_b(530)$ | $Y = 0.74 \cdot X$ | 0.99 |
| *R*rs(443) *vs* $\frac{b_b(450)}{a_w(443)+a_{t-w}(443)+b_b(450)}$ | $Y = 0.0496 \cdot X$, for $R\text{rs}(443)_{\text{model}}$ | 0.94 |
| | $Y = 0.0485 \cdot X$, for $R\text{rs}(443)_{\text{data}}$ | 0.90 |
| *R*rs(532) *vs* $\frac{b_b(530)}{a_w(530)+a_{t-w}(530)+b_b(530)}$ | $Y = 0.0533 \cdot X$, for $R\text{rs}(530)_{\text{model}}$ | 0.96 |
| | $Y = 0.0498 \cdot X$, for $R\text{rs}(530)_{\text{data}}$ | 0.98 |
| *R*rs(670) *vs* $\frac{b_b(650)}{a_w(670)+a_{t-w}(670)+b_b(650)}$ | $Y = 0.057 \cdot X$, for $R\text{rs}(670)_{\text{model}}$ | 0.96 |
| | $Y = 0.058 \cdot X$, for $R\text{rs}(670)_{\text{data}}$ | 0.94 |
| $b_b(450)$ *vs* *R*rs(443) | $Y = 34.06 \cdot X - 0.02$ | 0.67 |
| $b_b(530)$ *vs* *R*rs(532) | $Y = 12.63 \cdot X - 0.017$ | 0.77 |
| $b_b(650)$ *vs* *R*rs(670) | $Y = 15.82 \cdot X - 0.008$ | 0.88 |
| $b_b(650)$ *vs* $a_{nap}(412)$ | $Y = 0.0463 \cdot X - 0.0092$ | 0.76 |
| $b_b(650)$ *vs* $a_{nap}(380)$ | $Y = 0.0411 \cdot X - 0.0107$ | 0.83 |
| [chl-a] *vs* $b_b(650)$ | $Y = 433.5 \cdot X - 0.92$ | 0.57 |
| $a_{nap}(412)$ *vs* *R*rs(670) | $Y = 302.2 \cdot X + 0.159$ | 0.70 |
| $a_{nap}(380)$ *vs* *R*rs(670) | $Y = 356.71 \cdot X + 0.168$ | 0.74 |

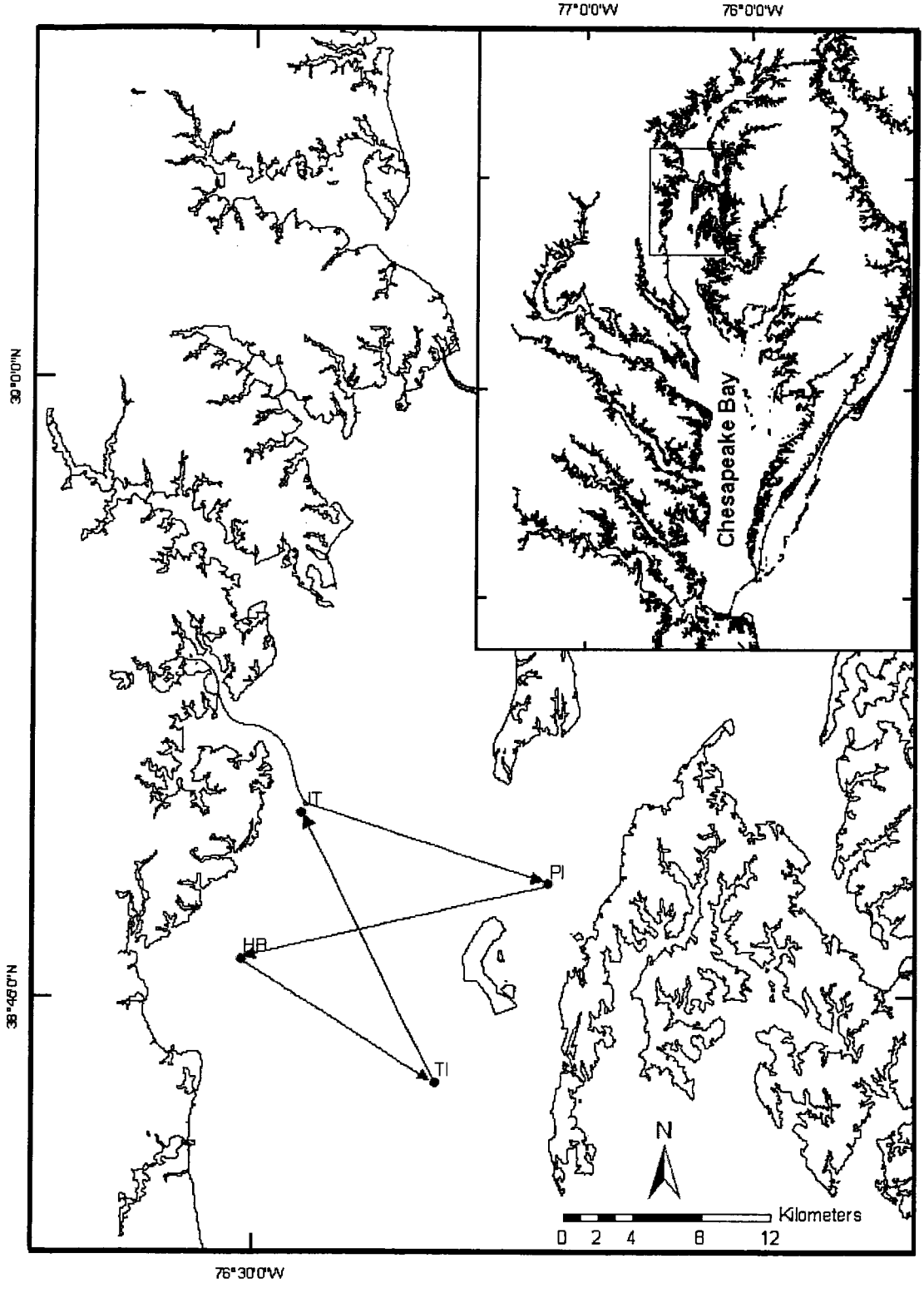


Figure 1, Tzortziou et al.,

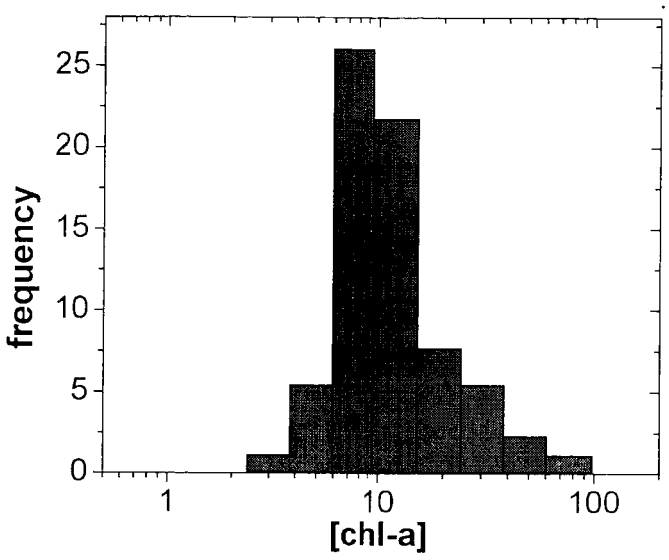


Figure 2, Tzortziou et al.,

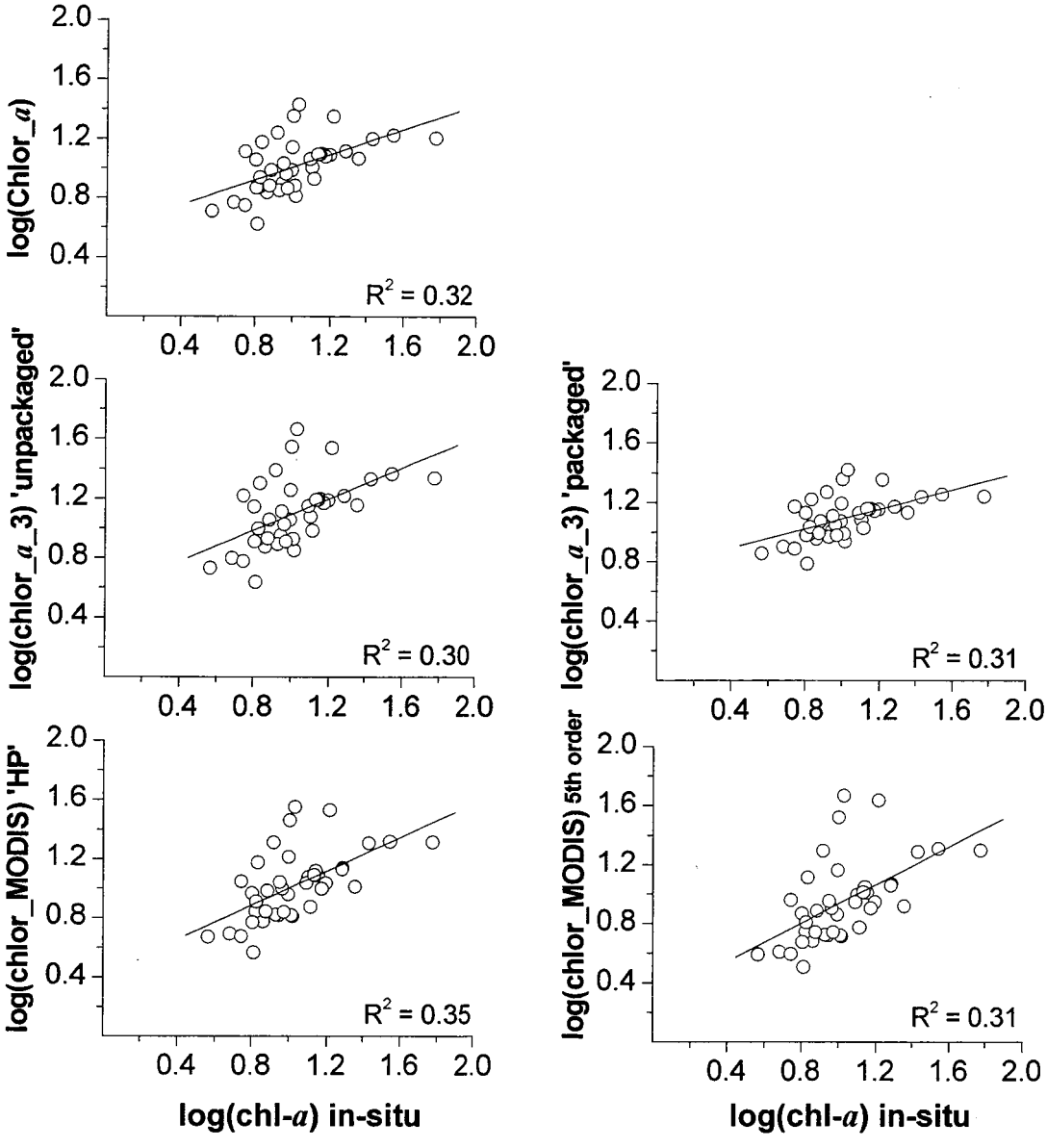


Figure 3, Tzortziou et al.,

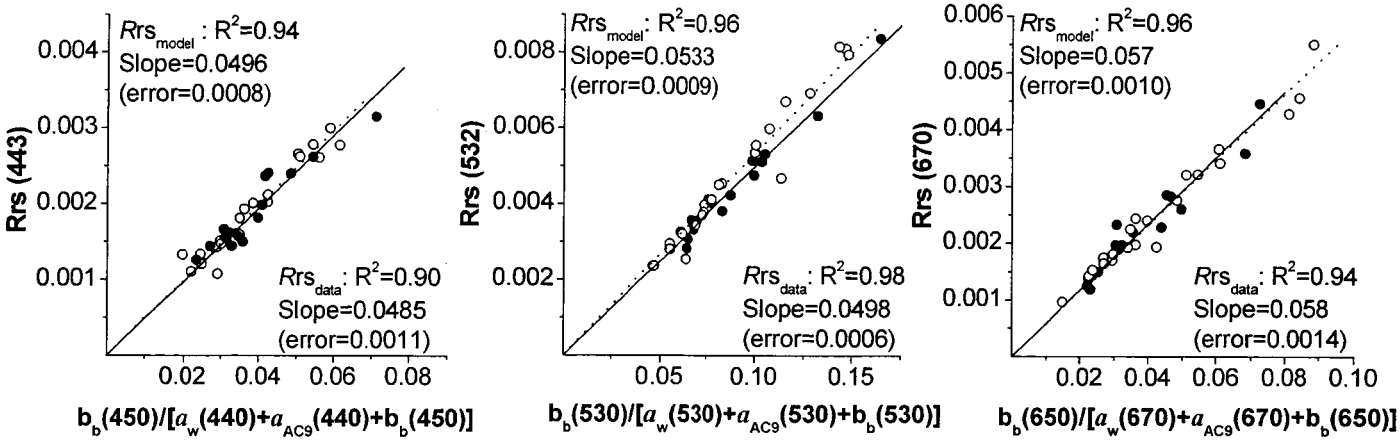


Figure 4, Tzortziou et al.,

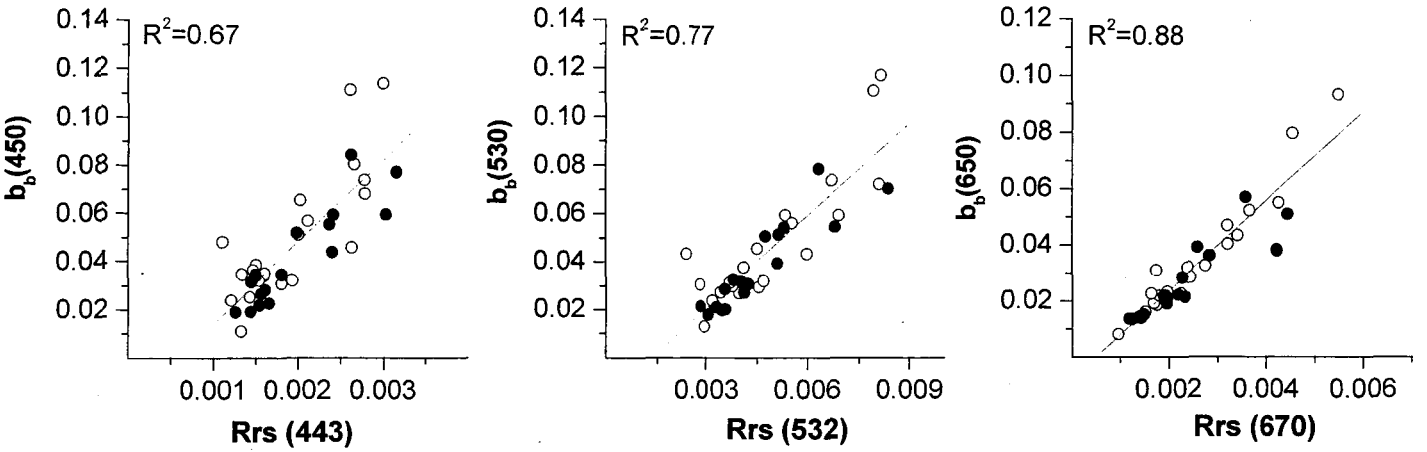


Figure 5, Tzortziou et al.,

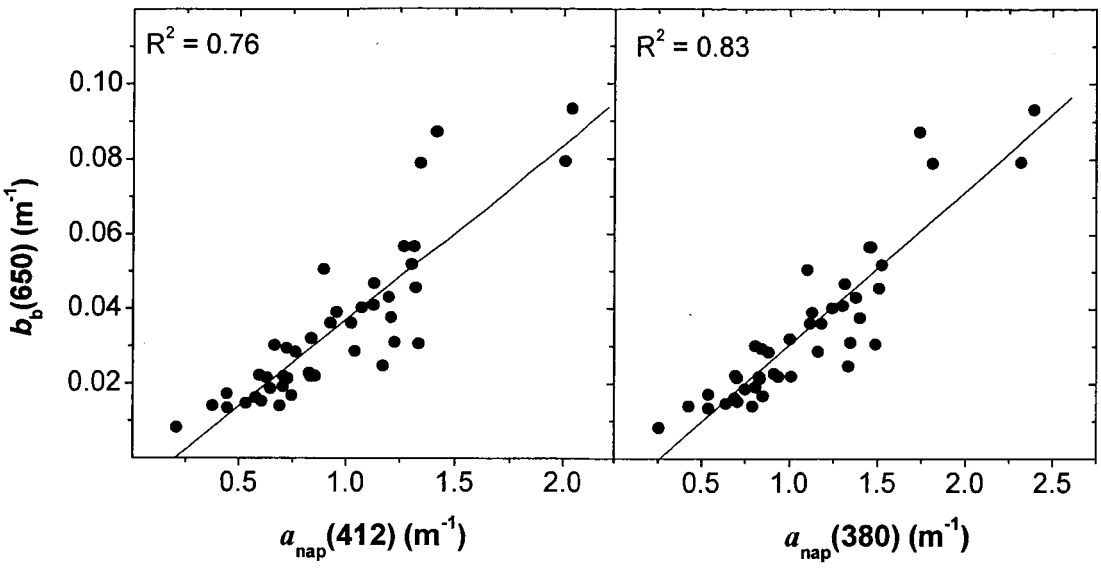


Figure 6, Tzortziou et al.,

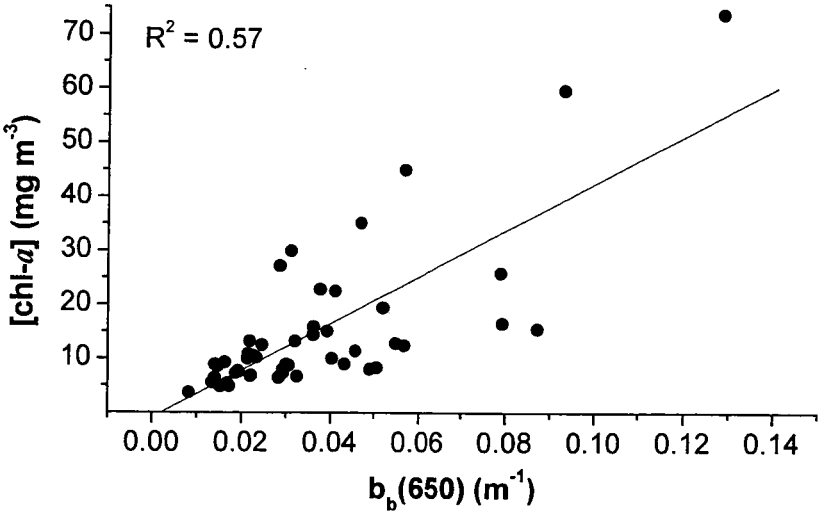


Figure 7, Tzortziou et al.,

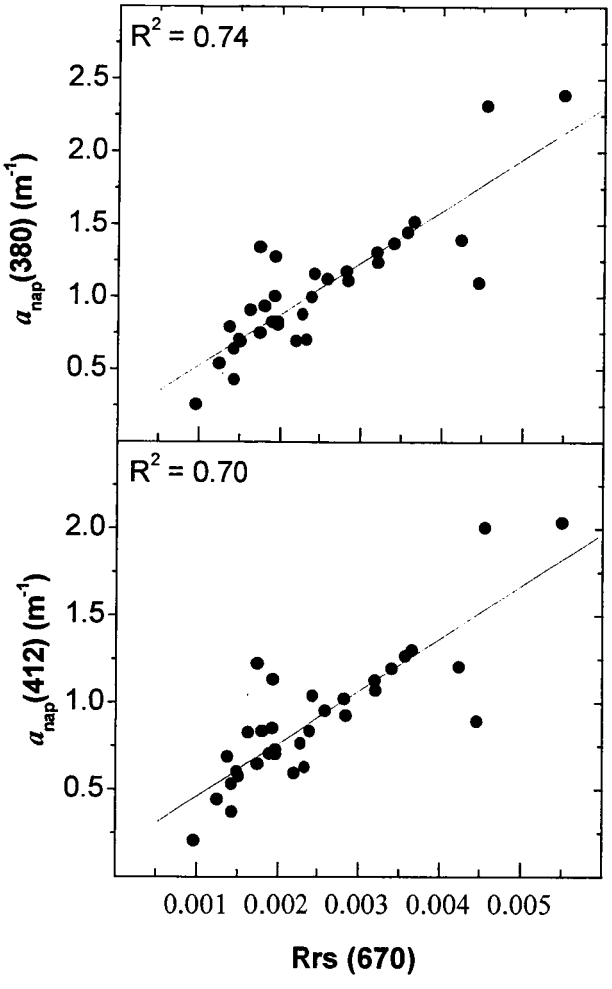


Figure 8, Tzortziou et al.,

## Popular Summary:

The particulate and chemical composition of the ocean and their concentrations can be measured from satellites by monitoring the color of the water. Interpretation of the measured color is still a major problem, especially in coastal waters such as the Chesapeake Bay. Recently, we have shown how to combine theoretical models for the propagation of light through water with an extensive bio-optical database to examine the relative roles of light absorption and scattering from different substances that might be in the Chesapeake Bay. We applied the results to measurements just above the water's surface and to satellite using our derived relationships between remotely sensed quantities and optical properties of individual water components. We also evaluated methods for remote retrieval of the amount of chlorophyll and suspended inorganic particles.

Currently operational chlorophyll algorithms used by MODIS (MODerate resolution Imaging Spectroradiometer) are based on empirical relationships between chlorophyll concentration ([chl-a]) and blue-green remote sensing reflectance (Rrs) ratios. These algorithms break down in coastal waters because they do not sufficiently account for the effects that substances other than chlorophyll (i.e. non-living particles and dissolved organics) have on the color of the water. We show that relationships between [chl-a] and Rrs in the long visible wavelengths, where interference from non-living particles and dissolved organics is minimal, provide a better basis for satellite monitoring of phytoplankton blooms in these waters. Both our measurements and model simulations indicate that highly-refractive non-living, mainly inorganic, particles play a dominant role in regulating backscattering variability in the Chesapeake Bay waters. These results, in conjunction with our findings that backscattering in these waters can be estimated from the satellite measured Rrs at 670 nm, suggest that satellite ocean color can be applied to remotely monitor distribution and concentrations of highly refractive inorganic suspended particles in the Chesapeake Bay. Also, our results are the first showing that satellite measurements can be used to separate the contribution by non-living particles and dissolved organics to the total light absorption in the blue wavelengths. Separating the contribution by these two separate, but similarly absorbing, components to total light absorption is particularly useful for studies on dissolved organic carbon cycling in the coastal zone.